

# How fast can it go?

## *Rapid lake-ecosystem responses to catchment processes during the Copper Age at Lago Grande di Avigliana (Northern Italy)*



**Thierry R. Fonville**<sup>1</sup>  
**Walter Finsinger**<sup>2</sup>  
**Emiliya P. Kirilova**<sup>1</sup>  
**Lucas J. Lourens**<sup>3</sup>  
**André F. Lotter**<sup>1</sup>

1

Laboratory of Palaeobotany and Palynology  
Institute of Environmental Biology  
Faculty of Science  
University of Utrecht

2

Centre de Bio-Archéologie et d'Écologie (UMR 5059, CNRS)  
Institut de Botanique  
University of Montpellier II

3

Faculty of Geosciences  
Department of Earth Sciences  
University of Utrecht



## Contents

Abstract .....	2
Preface.....	3
Introduction.....	5
Varved sediment in carbonate rich lakes .....	5
Eutrophication.....	6
Fire Regime.....	6
Post-glacial climate.....	7
Study Area .....	8
Material and Methods.....	9
Sediment coring .....	9
Floating chronology.....	9
Sediment description and sampling strategy.....	11
Physical and geochemical proxies .....	12
Terrestrial and aquatic indicators .....	12
Results .....	15
Physical and geochemical proxies .....	15
Terrestrial and aquatic indicators - Macrocharcoal records .....	18
Aquatic indicators - Diatom analyses .....	24
Discussion .....	27
Physical and geochemical proxies .....	27
Terrestrial indicators - Vegetation dynamics .....	27
Terrestrial indicators - Macrocharcoal-inferred fire regime .....	28
Terrestrial indicators - Fagus dynamics.....	29
Aquatic indicators - Diatom dynamics.....	30
Sediment runoff dynamics and influence on lake ecosystems .....	32
Lake level fluctuations and climate change .....	33
Conclusions.....	34
Literature.....	35

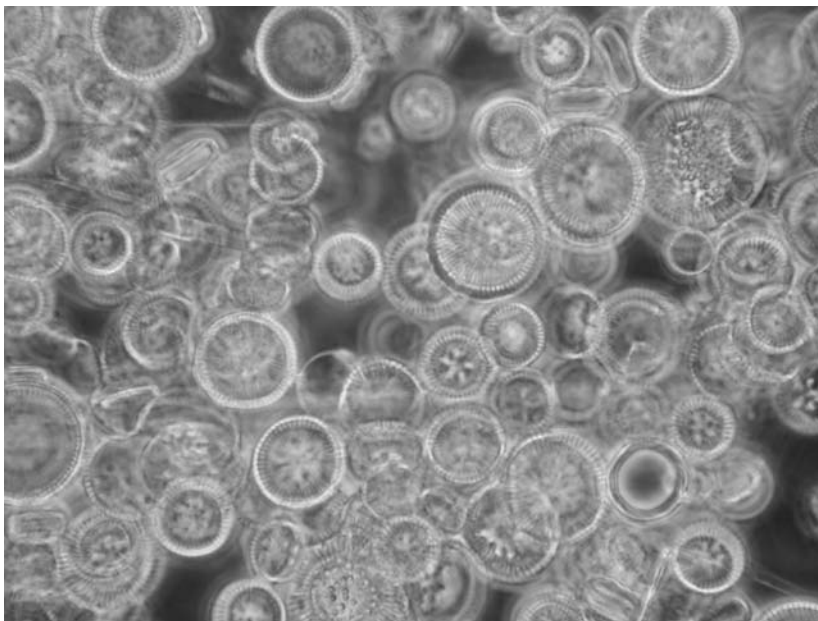
## **Abstract**

Over the past decades, increasing effort has been spent on understanding the effects of recent cultural eutrophication of European waters. However, simply reverting to conditions ~150 years ago is generally insufficient since both human activities and natural climate changes have influenced the landscape and nutrient levels of rivers and lakes for several millennia. Limnological, geochemical and terrestrial ecological records ( $\mu$ XRF, LOI, pollen, macrocharcoal and diatom analyses) were collected from an annually laminated lake sediment (sampled at a contiguous 15 yr resolution) to investigate the resilience of lake ecosystems under natural and pre-industrial conditions. We focus on a sediment section that contains ~1600 years and which includes an abrupt transition to darker, organic-rich sediments at 4800 cal. yrs BP (Copper Age). Pollen and diatom records suggest minimal changes in the terrestrial and aquatic ecosystems prior to the transition. Across the transition, no clear human impact was detected in the vegetation which appeared to be stable. However the fire regime indicates more frequent fires across the transition. Furthermore, a major change in lake water chemistry occurred as indicated by diatom assemblages and silica and diatom inferred total phosphorous (DI-TP). The ecosystem switched to a silica limited lake (low Si:P ratio). A climatic cause for this might be increased erosion, potentially driven by wetter conditions. However another cause might be extended ice cover during a colder period, leading to internal phosphorus loading due to extensive anoxia. Evidence for this cold period can be found in other Central European lake level studies. In conclusion, this study indicates a short term climatic interval, which has a major effect on the lake ecosystem. Furthermore the transition of the lake-ecosystem was rapid (~30 years) and showed a response similar to recent cultural eutrophication.

## **Preface**

Over the last year I have spent a lot of time developing my skills as a researcher. I knew in advance that it would be a big project which would require a lot of time and effort. There were times when I felt lost and unable to grasp the various processes contributing to a lake ecosystem. But I found it vary rewarding to be able to implement the multi-proxy approach in this thesis. I would not be able to accomplish this thesis without continued support and patience of my supervisors.

I would like to thank Walter Finsinger for his unending curiosity, always asking the questions which help me solve difficulties. His high spirit helped me through the periods when I felt overwhelmed by the amount of work. I would also like to thank him and Verushka Valsecchi for providing a home away from home during my stay in Montpellier. Andy Lotter has my thanks for keeping my mind sharp, helping my interpretation and the occasional push to achieve a higher level of research. His excellent analytical mind and vast experience helped me evaluate the various proxies and spot potential pitfalls. Emiliya Kirilova has my gratitude for helping me understanding the diatom assemblages and the limnological mechanisms behind it. Also for checking up my progress and making sure I would like to thank Volker Wennrich from the University of Cologne for the XRF analysis. The Palaeoecology Group in Utrecht has provided a warm home for my scientific development with an enthusiastic atmosphere. Extended thanks to the student group of Palaeoecology, for the nice conversations about just about anything. I would like to thank the Centre de Bio-Archéologie et d'Ecologie in Montpellier for welcoming me during the charcoal analysis and in particular Sandrine Subitani and Adam Ali for help with the macrocharcoal analysis and interpretation. I would like to thank Jan van Tongeren and for his help with the pollen and diatom preparations in Utrecht. Hans van Aken has my thanks for his assistance with the varve counting and LOI analysis and Sander van der Pot for his help with the LOI.



*Photograph of analyzed, pre-transition diatom slide containing primarily Cyclotella species.*



## Introduction

Lake sediments provide long-term records of various events which take place in terrestrial and aquatic ecosystems. While the long-term history of human activities, such as forest clearing and eutrophication, and of natural induced changes (solar forcing, climate change) have been intensively studied in Europe, long-term records of the impacts of early land-uses on lake ecosystems are rare (Smol 2008).

In this study, we specifically aimed at estimating the response time of a lake ecosystem to landscape changes in the catchment area. This is achieved by analyzing an approximately 4800 year old sediment transition of a lake located in Northern Italy. The analyzed sediment consists of an abrupt sediment-colour transition from carbonate rich to organic rich varved sediments that was dated to ca.  $4820 \pm 220$  cal. BP by means of correlation of pollen zones (more details in the section '*floating chronology*'). The section was analyzed at high-resolution (a 15 year period) by a multi-proxy approach. To reconstruct changes in the terrestrial ecosystems (vegetation, fire regime) we used pollen and charcoal analyses and geochemistry and to assess the lake-water chemistry we used diatom analyses, and diatom inferred total phosphorus concentrations.

### *Varved sediment in carbonate rich lakes*

Varved sediments allow for an extremely precise age assessment, since they consist of seasonal layers. Seasonal cyclic events trigger the formation of either darker organic rich or brighter sediments (O'Sullivan 1983; Lotter and Birks 1997). The driving factor behind the formation of annual sediment layers is the amount of mixing in the lake waters and at least seasonal anoxic conditions at the lake bottom which will prevent the mixing of the sediments due to bioturbation (e.g. O'Sullivan 1983). In the case of carbonate rich lakes, the high epilimnic production during spring and summer causes a supersaturation of carbonate in the hypolimnion (bottom of the lake). Photosynthesis of phytoplankton (diatoms, green algae) in the photic layer is considered to cause substantial depletion of  $\text{CO}_2$ , increasing carbonate ( $\text{CO}_3^{2-}$ ) levels in the lake (due to chemical balancing) and thus  $\text{CaCO}_3$  precipitation (e.g. O'Sullivan 1983; Thompson et al. 1997). Increased precipitation and melting snow during spring will cause increased mixing in the lake, allowing organic matter to be transported deeper in the lake. Combining the above mechanisms a bright, calcite rich layer is created during spring and summer. During winter the combined effect of reduced melt water influx and lake surface freezing reduces the mixing substantially, increasing anoxia in the hypolimnion. This creates a dark, organic rich layer since the oxygen is quickly depleted by decomposition requirements in the layers above the hypolimnion. Thus on a yearly basis a dark and a bright layer are deposited, which may be used as a yearly age scale.

### *Eutrophication*

Eutrophication is a natural process, which indicates the maturation of a lake ecosystem (Whiteside, 1983; Smol 2008), where production increases due to higher nutrient levels. This occurs in many high depositional environments or ephemeral influx systems. The dilution and mobility of nutrients can in turn be controlled by climate, for example changes in temperature can have a strong effect on the evaporation/transpiration ratio, the length of ice cover, but also on the catchment area, thus influencing the nutrient state of a lake (e.g. Schindler 1996; Kirilova et al. 2009). On the other hand, human activities have been influencing landscape in many ways (Messerli et al. 2000). One important aspect of this is the creation of cultural lands to yield crops and grazing meadows, which can lead to high nutrient concentrations in surface and ground waters (Dearing et al. 2006). Thus cultural eutrophication has become a major environmental issue for most of the freshwater ecosystems in the world (Smol 2008). The combined effect of climate and land-use changes can lead to an increased risk of cultural eutrophication via nutrient loading through agriculture, industry, sewage release, and soil erosion (Schindler et al. 1996). Eutrophication of lake ecosystems can influence hypolimnetic anoxia. Higher production rates will increase the amount of organic matter sinking to the bottom of the lake, which will increase oxygen consumption by respiration (Antoniades 2007).

When attempting to investigate the resilience of lake ecosystems to land-use and climate changes, the limited availability of long-term monitoring data is a major concern (e.g. Lotter et al. 1997; Finsinger et al. 2006). Hence, little is known as to the response time and the rate of change of lake ecosystems to climate, land use changes, and natural disturbances (e.g. forest fires) under low-human impact conditions. Such knowledge might be useful to estimate the sensitivity of lake ecosystems to minor disturbances. Already a few studies have been performed on lake sediments showing the extent of eutrophication during pre-industrial times (e.g. Moser et al. 2002; Finsinger et al. 2006).

### *Fire Regime*

Forest fires can originate from natural sources, such as drought or high temperatures, but also from anthropogenic activities (e.g. Clark 1990; Whitlock and Larsen 2002; Carcaillet 2007). Fire has been used by early farmers to create openings in the forested landscapes for agriculture (Pott 1998). Any charcoal particles found within lake samples might be not only be an indication of human impact, but also of climatic changes. Land-use changes can have profound effects on forest cover and on forest fire regimes, both of which can lead to eutrophication because they increase erosion and nutrient input into lakes (Bradbury 1986; Kelly et al. 2006). Commonly it was assumed it is best to leave nature to itself as much as possible, as that would establish climax vegetation (e.g. Clements, 1936; Odum, 1969). However this means that fire prone regions, such as southern Europe, will be often subject to fires (Tinner et al. 1999). Since many parts of this region can be heavily populated, further research is needed to get a better indication of the response of vegetation to the fire regime and to get an idea of the natural fire regime. Vegetation analysis can give further insights into the forest response to the fire events and is important to support the charcoal proxies. A few studies (e.g. Tinner et al. 1999; Tinner et al. 2000) indicate that some shrub species (i.e. birch, hazel) have a preferential response to fire events, while some evergreen species (i.e. fir, ivy) are fire intolerant. A more recent assumption is that evergreen oak is actually hindered by fire events (Colombaroli et al. 2007). Macrocharcoal is assumed to reflect local fire event, as opposed to microscopic charcoal (Carcaillet et al. 2001). Though a recent study indicates that during exceptionally large fire events large pieces of charcoal can travel several kilometres (Tinner et al. 2006).

### *Post-glacial climate*

To understand some of the long term mechanics driving the vegetation, some background is given about the long term climate trends. During the Last Glacial Maximum the ice-sheet cover of the Northern Hemisphere continents were at their maximum. This was about 21,000 cal. BP. After this the climate started to warm up again (Ruddiman 2001). This warming is briefly interrupted by a Heinrich events (short cold periods, indicated by Ice Rafted Debris, e.g. Broecker 1994) and a cold reversal lasting about 1300 years, which is called the Younger Dryas (YD) event (e.g. Rodbell 2000). Evidence of the YD event came initially from European pollen records, which showed an invasion of cold-tolerant herb tundra starting around 13,000 cal. BP (Starkel 1991). During this time many frost intolerant tree-species were driven into refugia in Southern Europe. This cold oscillation lasted until about 11,700 years ago, which marks the beginning of the Holocene. Following the onset of the Holocene, the climate warmed up with highest temperatures reached around 6000 cal BP, though the timing and extent of this warming varied regionally (Wanner et al. 2008; Renssen et al. 2009). High-resolution studies that focussed on Holocene climate variability in central Europe (e.g. Haas et al. 1998; Heiri et al. 2003; Vollweiler et al 2006) indicate that the European climate fluctuated intensely.

### *Holocene Archaeology*

Human development can be divided into several stages, but differs locally. The Neolithic (New Stone-age) started around 7550 cal. BP in Northern Italy (Pessina 2000). The period between the end of the Neolithic and the start of the Bronze Age is called the Copper Age (or Calcolithic), stretching from about 5500 until about 4100 cal. BP. The Holocene archaeological record attests to the presence of human civilizations in North-western Italy.

In comparison to other European regions, there is a lack of high resolution vegetation reconstructions from archaeological findings dating back to before the Bronze Age, when human activities intensified. In a previous study, Rottoli and Castiglioni (2009) noted that although information about many Neolithic and Chalcolithic settlements has increased over the past decades, the resulting data was still scarce (Figure 1) and with inadequate sampling. Besides evidence for the cultivation of cereals, they found that acorns, hazel nuts and grapes were an important part of the Neolithic diet. Although few settlements were found in Northern Italy, it is impossible to rule out the influence of human activities since the Middle Neolithic in shaping the landscapes of the region. However during the Bronze Age, human activities intensified drastically, as can be seen in the reconstructed vegetation of several sites in the Southern Alpine region (e.g. Finsinger and Tinner 2006; Valsecchi et al. 2008).

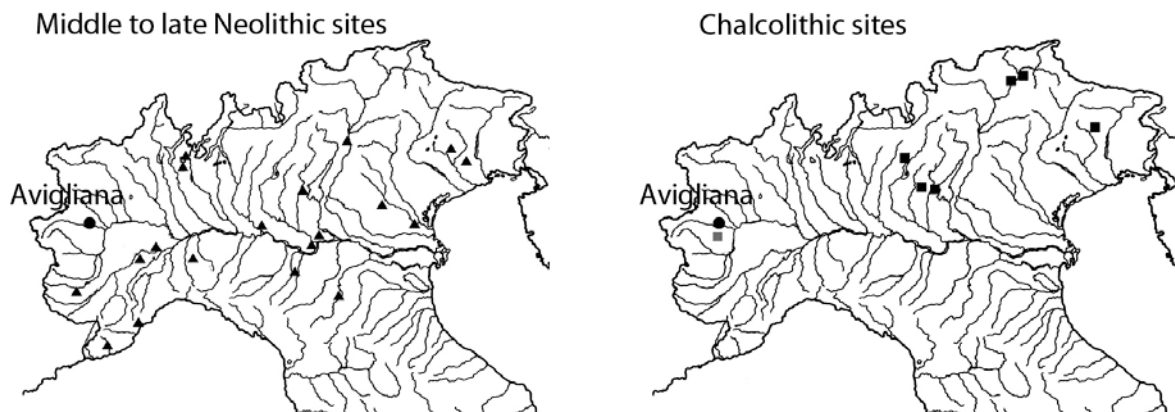


**Figure 1: Middle to Late Neolithic (c. 5100/4500–3500 cal. B.C.) and Chalcolithic (c. 3500–2100 cal. B.C.) archaeological sites in Northern Italy. After Rottoli and Castiglioni (2009).**



## Study Area

Lago Grande di Avigliana (AVG, 45°03'54" N, 07°23'12" E, 352m asl) is a circular lake located in the southern forelands of the North western Alps west of Turin (Figure 2, Table 1). The surrounding landscape was shaped by the Val di Susa glacier that reached probably at the Last Glacial Maximum the northern shore of the lake, where it deposited a terminal moraine. The lake is fed by two seasonal streams and by the outflow of Lago Piccolo di Avigliana, which is located south of Lago Grande di Avigliana. From there water flows into the Torbiera dei Mareschi and eventually into the Dora Riparia River, the main river in the Val di Susa valley. Bedrock in the catchment is composed of metamorphic rocks that are often covered by weathered till deposits (Petrucci et al. 1970). At present the region is characterized by a temperate mid-latitude climate without any dry season. Precipitation is currently about 800 mm year<sup>-1</sup> with maxima occurring in spring and autumn (Biancotti et al. 1998). Most of the catchment is covered with a mixed oak forest (oak, alder, elm, chestnut). 25 years ago this lake was deemed the second most eutrophicated lake in Italy, at that point the total phosphorous (TP) concentration was ~225 µg l<sup>-1</sup> (n=147, Gaggino et al. 1985). Sewage discharge since the 1950's led to eutrophic and hypertrophic conditions culminating in the 1960's. Starting in the 1980's the sewage water was deflected, leading to somewhat of a recovery (~100 µg l<sup>-1</sup>). Since 1994 nutrient rich hypolimnetic water is actively being pumped out of the lake, further reducing the TP concentration of the lake to about 40 µg l<sup>-1</sup> (Finsinger et al. 2006).

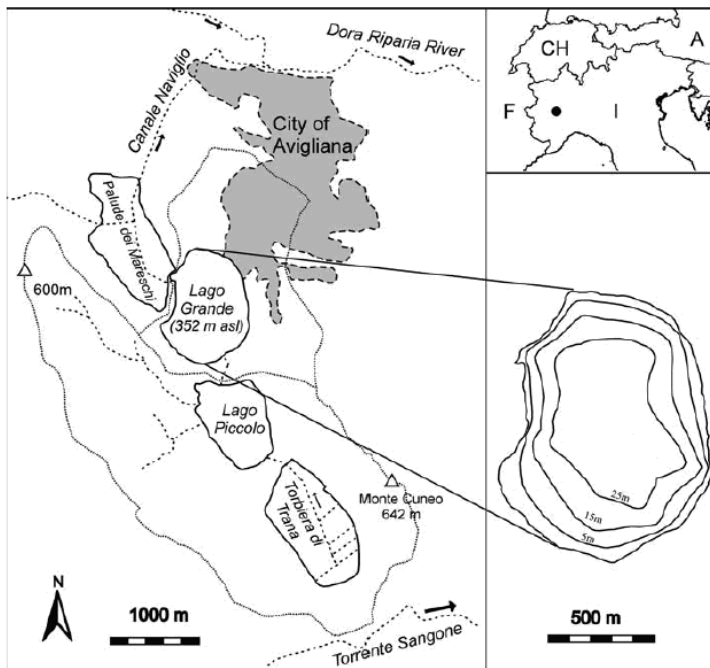


Figure 2: Location of the study area (after Finsinger et al. 2006).

**Table 1: Morphometric, physical and hydrochemical features of AVG (after Gaggino and Cappelletti 1984, from Finsinger et al. 2006)**

Elevation (m asl)	352
Lake surface (km <sup>2</sup> )	0.83
Catchment area (km <sup>2</sup> )	10.7
Length of shore line (km)	3.6
Maximum depth (m)	26
Mean depth (m)	19.5
Maximum length (km)	1.2
Maximum width (km)	0.8
Lake volume (10 <sup>6</sup> m <sup>3</sup> )	16.2
Theoretical Renewal Time (years)	2.3
Winter-ice cover	irregular
Mean pH	7.6
Min–Max TP (µg P l <sup>-1</sup> )	53–704
Alkalinity (meq l <sup>-1</sup> )	2.54
Conductivity (µS cm <sup>-1</sup> )	260

## Material and Methods

### *Sediment coring*

Sediments from AVG were obtained in 2004 using a piston corer that was operated from a floating platform (UWITECH) anchored on the lake's centre (at ~25 m water depth). Two sets of parallel cores were taken at ca. 50 m distance from each other. Each of the two sets consists of two cores that were taken with an overlap of ~ 50 cm, so as to guarantee the full recovery of drive intersections. The sediment drives (3 m length and 5.7 cm in diameter) were cut on the platform into 1 m long segments and thereafter transported to the lab, where they were cut longitudinally, photographed, packed in plastic foil, and stored at 4 °C in a cool box. Subsequently, the sediment segments AG004\_II and AG010\_II have been cut into slices comprising 15 years. Each slice was sub-sampled by cutting polygons of 1 cm<sup>2</sup> surface for further analyses, (similar to O'Sullivan 1983). Only selected subsamples (see '*Sediment description and sampling strategy*') were used for: 1) pollen analysis, 2) macrocharcoal analysis, 3) LOI, and 4) diatom analysis. The remainder of each slice was stored to allow future studies. All subsamples were freeze-dried prior to processing.

### *Floating chronology*

A floating chronology was established based on varves, which were counted under a stereomicroscope at x15 magnification. The light spring/summer carbonate-rich layers were counted in increments of 5 mm depth by two separate analysts in order to allow an estimate of the counting accuracy.

The composite stacked record was made possible by synchronization of distinct marker beds in both segments (see Figure 3 and Table 2).

The age of the transition coincides with the expansion of *Fagus sylvatica* (beech). This is correlated to pollen stratigraphy of Lago Piccolo di Avigliana (Finsinger and Tinner 2006). The onset of *Fagus* pollen increase is correlated to the transition between pollen zones LPAZ AVP-9 to LPAZ AVP-10 (yielding an estimated age of 4820 ± 220 cal. yrs BP (2870 ± 220 cal. yrs BC).

The ages used in this report are all in varve years before the transition (yrs BT). The ages referred to are the mid-point ages. So a sample that has an age of 0 yrs BT actually ranges from 7.5 to -7.5 yrs BT and a sample with a midpoint of 90 years following the transition has an age of -90 yrs BT. By adding this relative age to the transition age it is potentially possible to derive an estimated age in cal. yrs BP or BC.

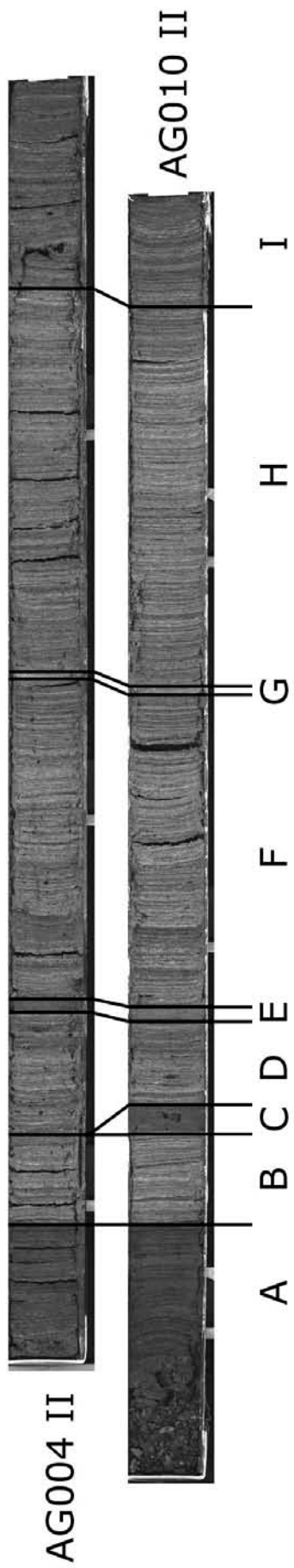


Figure 3: Core images displaying some of the major marker beds. The individual cores have a length of ~1m. See table 2 for more details about the layers (A-I). The line between layers A and B indicates the colour transition.

### Sediment description and sampling strategy

In the cores several distinct turbidites appear (table 2: silty grey layers, labelled C, E and G) that were used to correlate the core segments to each other. During the sediment sub sampling, it was chosen to avoid a thick turbidite (layer C) in core AG010II, located at ~27-29 cm, by switching to core AG004II. Another turbidite (at ~27 cm depth in core AG004) was excluded from the analysis (layer E), since it is assumed that it was deposited during a short period of time (days or weeks) and has thus little influence on the age scale (e.g. Lamoureux and Bradly 1996) following the transition. The oldest turbidite (thin grey layer) was thin (~2mm) and included in the sample with an age of 750 yrs BT.

Samples analysed for pollen, diatoms, macrocharcoal, and loss-on-ignition were selected from both core segments (Table 3). The composite record was established based on the correlations made. A composite depth (sample transition depth), where the zero value was set at the sediment-colour transition, was then associated to each sample after subtracting the large turbidites (marker beds labelled C, E). As layer G was too thin, it was included in the sample (sample mid-age ~750 yrs BT). Sediment samples that were not analyzed were stored.

**Table 2: Sediment description.**

Label	Description	AG010 sample mid-depth (cm)	AG004 sample mid-depth (cm)	Transition sample mid-depth (cm)	Sample mid-age (yrs BT)
A	brownish/dark varves	0-15.3		<b>Not sampled</b>	<b>Not sampled</b>
	brownish/dark varves	15.3-20.4		-5.1-0	-150-0
B	greyish/bright varves	20.4-26.4		0.65-6	15-150
C	thick dark grey layer	~27-29		<b>Not sampled</b>	<b>Not sampled</b>
D	greyish/bright varves		19.9-20.75	6.8-7.65	165-180
		30.4-34.35		8.3-12.25	195-285
			26.45	13.05	300
E	thick grey silty layer		27.55	14.15	308
F	greyish/bright varves		28.7-29.55	15.3-16.15	315-330
		39.3-47.6		16.9-25.2	345-510
			40.1-50.5	25.9-36.3	525-705
	60.05-60.65		37.05-37.65	720-735	
G	thin grey silty layer	61.4		38.4	750
H	greyish/bright varves	62.1-86.35		39.1-63.35	765-1245
			78.8-82.4	64.67.6	1260-1335
I	greyish/darker varves	91.5-95.7		68.2-72.4	1350-1455
		95.7-100		<b>Not sampled</b>	<b>Not sampled</b>

**Table 3: Composite record, calculated transition depth and ages.**

Core	Label	Depth within core segment (cm)	Sample mid-age (yrs BT)	No. of samples	Sample transition mid-depth (cm)
AG010_II	A/B	15.3 - 26.4	-150 - 150	21	-5.1 - 6
AG004_II	B	19.9 - 20.75	165 - 180	2	6.8 - 7.65
AG010_II	D	30.4 - 34.35	195 - 285	7	8.3 - 12.25
AG004_II	D/F	26.45 - 29.55	300 - 330	3	13.05 - 16.15
AG010_II	F	39.3 - 46.7	345 - 510	12	16.9 - 25.2
AG004_II	F	40.1 - 50.5	525 - 705	13	25.9 - 36.3
AG010_II	F/G/H	60.05 - 86.35	720 - 1245	36	37.5 - 63.35
AG004_II	H	78.8 - 82.4	1260 - 1335	6	64 - 67.6
AG010_II	I	91.5 - 95.7	1350 - 1455	8	68.2 - 72.4

### *Physical and geochemical proxies*

The inorganic element composition of the sediments was determined on unprepared core halves using an ITRAX X-ray fluorescence (XRF) core scanner (Cox Analytical Systems) (Croudace et al. 2006). The ITRAX was equipped with a 3kW Mo X-ray tube set to 30 kV and 30 mA to analyze semi-quantitative variations of elements from Al to U. XRF-scanning was performed at 500  $\mu\text{m}$  (AG010\_II) and 1 mm resolution (AG004\_II) and an exposure time of 20 s. Element amounts were presented as count rates as estimates of the relative concentrations in the sediment. Detection limits of the ITRAX range between 2.2% for Al and 5ppm for heavier elements like Sr or Rb (Croudace et al. 2006).

Sediment radiographs of the cores were made at 200-micron resolution, running the scanner with a voltage of 55kV, a current of 35mA, and an exposure time of 500/600ms. The XRF records are displayed as counts per second (cps). In this report the Si/Ti ratio is also used, which can be applied as an indicator of biogenic silica (Brown et al. 2007).

Magnetic susceptibility (MS) was measured on the split-core halves at 5 mm steps with a spot-reading logging sensor (MS2E, Bartington Inc.). Prior to logging and covering with plastic foil, sediment surfaces were cleaned carefully so that the measurements are not biased by material smeared along the split-surface. The drift of the sensor was monitored each 20 readings of the sediment by taking readings against air. The drift was subsequently modelled using a robust loess smoothing function (Cleveland 1979) (span = 0.5) and subtracted from the readings on the sediment, following Nowaczyk (2001). Of the two sediment segments analysed in this study, MS is available only for the segment AG004II. Since the age scale of the record is based on a floating chronology of both cores, samples which should have MS data from core AG010II have been replaced with MS data from core AG004II. To achieve this, the points between marker beds were interpolated to allow a good estimation of the MS at the same age.

For the greyscale analysis, high-resolution colour photographs were taken every 15 cm (with a 5 cm overlap) with a digital camera under homogeneous light conditions. These pictures were subsequently merged with Adobe Photoshop before transforming them to greyscale images and plotting a greyscale profile of the sediments with the ImageJ v 1.41o software (<http://rsbweb.nih.gov/ij/>). Greyscale values were measured each pixel (~ 50 pixels/cm depth) and averaged over 3 cm sediment width in order to minimize the influence of small cracks on the sediment surface.

Loss-on-ignition (LOI) was measured following Heiri et al. (2001). LOI at 550°C and LOI at 950°C were used to estimate the amount of organic matter and the amount of carbonate content, respectively. The remaining sediment after these two heating steps contains mostly clastic material and biogenic silica.

### *Terrestrial and aquatic indicators*

For the macrocharcoal analysis, samples were first treated with HCl (3%) at room temperature, then gently sieved with a 150  $\mu\text{m}$  mesh size, washed, and subsequently mildly treated with 2.6% bleach ( $\text{NaPO}_3$ )<sub>6</sub>, following Carcaillet et al. (2001).

Macrocharcoal particles were counted and measured using the program WinSeedle v2009a (Regent Instruments Inc.). The Fire Return Interval (FRI) was calculated using the program CharAnalysis v1.0 (Higuera et al. 2008), using a 400 yr background smoothing and 500 yr FRI smoothing, to allow interpretation of fire-regime changes (see results section for further details).

Pollen samples were prepared following physical and chemical treatments, stained, and mounted on microscopic slides following Lotter (1988). At least 300 pollen grains have been counted in each sample at x400 magnification and identified with pollen keys and atlases (e.g. Beug 2004; Moore et al. 1991). Exotic marker grains (*Lycopodium*, batch 483216) were added to the samples to allow the calculation of pollen concentrations, following Stockmarr (1971). Pollen and diatom percentage data was sorted from bottom left to top right using the software TRAN v1.8 (Lotter and Juggins 1991). Zonation was performed on taxa occurring in at least 4% of the samples and a minimum abundance of 0.75%. Zones were determined by optimal partitioning (Birks and Gordon, 1985) using ZONE 1.2 (Lotter and Juggins 1991) and the number of statistically significant zones was obtained by comparison with the broken-stick model (using BSTICK 1.0) following Bennett (1996). To give some statistical backbone to the vegetation interpretation, a Principal Component Analysis (PCA) analysis was performed. To test whether a PCA was possible, a Detrended Correspondance Analysis (DCA) was performed. Since this revealed a standard deviation gradient of 0.81, thus a PCA was applied (Ammann et al. 2000; ter Braak and Prentice 1988). The PCA was run using Canoco 4.5 for Windows. Unidentified pollen grains (Indeterminata and varia) were excluded from the ordination, since they were strongly correlated with the first axis and could not provide additional information. The first PCA axis explains 15.9% of the variance and the second axis 6.8%. Accumulation rates (AR; # particles cm<sup>-2</sup> years<sup>-1</sup>) of pollen, macroscopic charcoal (PAR and CHAR, respectively) and diatoms (valve AR) were calculated based on the sample integration time (SIT; # years) and the particle concentration (CONC; # particles cm<sup>-3</sup>) using the following formulas:

$$AR = CONC/SIT, \quad (1).$$

Concentration of pollen was inferred based on the ratio between 'counted' and 'added' exotic marker grains and counted pollen grains:

$$CONC = (\text{Added Exotic markers/Counted Exotic markers}) \times \text{Counted pollen}, \quad (2).$$

Since the sample surface (1 cm<sup>2</sup>) and the SIT (15 years) were determined by the sediment-subsampling strategy, the PAR is easily calculated using equations (1) and (2). Diatom accumulation is based on the split factor of the sample and the surface counted per slide. The accumulation rates remove interdependence of other species and allow a better reflection of species abundance. It was decided to standardize the PAR records, since the raw PAR record showed intensely fluctuating values, dominated by the total pollen accumulation rate. Z-score standardization was accomplished for each taxon by subtracting the mean and dividing by the standard deviation.

The diatom subsamples were treated with hydrogen peroxide in order to dissolve all organic carbon and with mild hydrochloric acid to remove all carbonate (following Battarbee 1973). Naphrax<sup>®</sup> was used as mounting medium. At least 300 valves were counted on random transects at 1000× magnification using an Olympus BX51 microscope equipped with an oil immersed objective and differential interference contrast. Diatom identification follows Krammer & Lange-Bertalot (1991, 1999a, 1999b, 2000). Valve accumulation rates (AR) were calculated for total number of valves, planktonic, periphyton and *Fragilaria* spp. valves and chrysophytes. Diatom Inferred Total phosphorus (DI-TP) concentrations are based on weighted averaging partial least squares (WA-PLS) regression and calibration (ter Braak et al. 1993; ter Braak & Juggins 1993) of square-root transformed diatom percentages and log transformed TP data and were calculated using the program C2 (version 1.5 Juggins 2007). The DI-TP model was developed from a combined European diatom data-base (EDDI, <http://craticula.ncl.ac.uk/Eddi/jsp/>) which consists of 429 sites and 577 diatom taxa. The modern TP concentrations range between 2 and 1189 µg L<sup>-1</sup>, with an average TP of 100 µg L<sup>-1</sup>. The bootstrapped 2-component WA-PLS inference model has a root mean square error of prediction (RMSEP) of 0.28 log TP units and a bootstrapped r<sup>2</sup> of 0.76.

Data was plotted using Tilia 2.0 and TGView 2.02 (Grimm 1991-2004).

## Results

### *Physical and geochemical proxies*

Between the 5mm increment countings of the separate analysts, there was a standard deviation of 1.6 varves on average. Especially in the post-transition darker varves in core AG010\_II, there was a higher discrepancy (>4 varves) between analysts.

Figure 4A shows the magnetic susceptibility (MS) changes measured on core AG004 II. At the bottom of the core the MS is low (around  $1 \times 10^{-6}$  SI) with a maximum around 1300 yrs BT. Following this the MS decreases again to low values and stabilizes around 950 yrs BT. High MS values can be seen around where the two turbidites occur (at 750 yrs BT and 308 yrs BT). From ca. 200 yrs BT the MS gradually increased reaching the highest values at the top of the sediment section. Across the transition the rate of MS change slightly increases.

Sediment colour, as inferred from the greyscale record (Figure 4B) shows a slight increase from values of ~100 to ~125 at 1350 years BT. Thereafter greyscale values are fairly stable with small fluctuations in the order of magnitude of ~10, and subsequently drop abruptly to values of ~75 at the transition (0 yrs BT). Smaller-amplitude minima in the greyscale record can be observed at around 400, 700, 800, 1000 and 1400 yrs BT. The geochemical records are displayed in figures 4c-f. The XRF-derived Calcium (Ca) content (Figure 5C) shows a rapid increase from 175k to 225k cps at ca. 1400 yrs BT, then Ca levelled-off at ~ 225k cps until ca. 900 yrs BT and thereafter gradually decreased to values around 175k cps around the layer G, 750 years BT. By contrast, in the turbidite deposited around 308 yrs BT (layer 'E') Ca cps do not decrease. Overall, Ca content gradually increases starting from ca. 750 yrs BT reaching values of ~ 350k cps at 150 yrs AT. Until the transition the XRF Iron (Fe) appears more or less stable around 10k cps. Deposition of the turbidite can be seen (layer G, 750 yrs BT, 20k cps) and a spike at 210 yrs BT (~35k cps). Following the transition the XRF Fe increases to 17.5k cps.

The Titanium (Ti) XRF cps (4E) shows overall stable concentrations, fluctuating around 500 cps. Around 1100 yrs BT there is a maximum of about 1500 cps. Around layer G there are two peaks (800 and 750 yrs BT), with values of 1000 and 1500 cps. The rest of the core shows low Ti values, fluctuating around 250 cps. The second turbidite (308 yrs BT) shows up as a minor increase, as does a maximum at -100 yrs BT (increases around 500-750 cps). The Silica (Si) as measured with the XRF analysis (cps, Figure 4F) shows a more or less stable record (values around 1500 cps) up to layer G, 750 yrs BT. There is a maximum around 1150 yrs BT and around this turbidite. Up till the transition there is a decreasing trend with two maxima, at 450 yrs BT and about 100 yrs BT. Following the transition there is a clear and rapid decrease towards less than 250 cps.

The Si/Ti ratio (Figure 4G) can be used to estimate the amount of biogenic silica in lacustrine sediments. From 1450-1100 yrs BT the Si/Ti ratio is somewhat decreasing. Up till the transition there are several maxima (900, 775, 450, 200 and 75 yrs BT) with a ratio of about 8. The turbidites (layer E and G, 750 and 308 yrs BT) are picked up as relatively low values (ratio 2). Following the transition the Si/Ti ratio decreases to about 1.



Figures 4H-Ji show the LOI fluxes ( $\text{g cm}^{-2} \text{yr}^{-1}$ ). The organic matter accumulation rate (Figure 4G) was more or less stable with values of  $\sim 0.2 \text{ g cm}^{-2} \text{yr}^{-1}$ . There are two distinct increases just before and at the layer E (400 and 308? yrs BT), where the organic matter flux increases till about  $0.35 \text{ g cm}^{-2} \text{yr}^{-1}$ . The maximum organic matter flux occurred just following the transition (-50 yrs BT), with an organic matter flux of about  $0.4 \text{ g cm}^{-2} \text{yr}^{-1}$ . Graph 4H shows the LOI  $\text{CaCO}_3$  flux, which is more or less stable at around  $0.4 \text{ g cm}^{-2} \text{yr}^{-1}$  up to about 0 yrs BT. There are maxima at 1200, 800 and 307 (turbidite 2) yrs BT, with values as high as  $0.6 \text{ g cm}^{-2} \text{yr}^{-1}$ . Following the transition the  $\text{CaCO}_3$  flux seems to slowly decrease towards  $0.3 \text{ g cm}^{-2} \text{yr}^{-1}$ . Figure 4I shows the LOI ignition residue (IR) flux, which appears stable around  $1.25 \text{ g cm}^{-2} \text{yr}^{-1}$  for most of the record. Maxima can be seen at 1200, 650 and 307 yrs BT. Following 100 yrs BT the IR flux slowly decreases to below  $0.5 \text{ g cm}^{-2} \text{yr}^{-1}$ .

Finally, Figure 4K is the stacked record of the percentage LOI data. It shows a doubling in the organic content when comparing the material below the transition ( $\sim 15\%$ ) to above the transition ( $\sim 30\%$ ). For the rest of the core the organic content remains more or less stable at about 15%. The carbonate content remains more or less stable ( $\sim 30\%$ ), though it does seem to decrease somewhat at the bottom of the core. The IR decreases above the transition and there is a small increase around 750 and 1250 yrs BT. Also at the bottom of the record the IR seems to decrease as well.

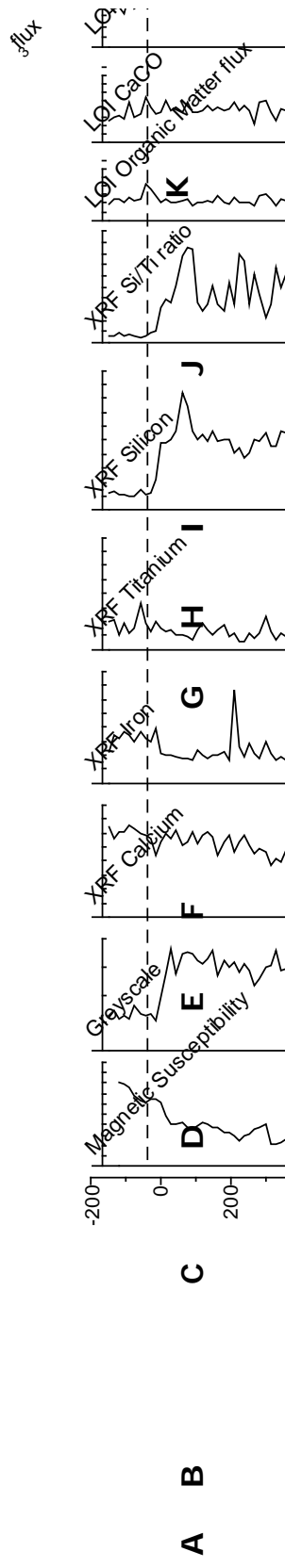
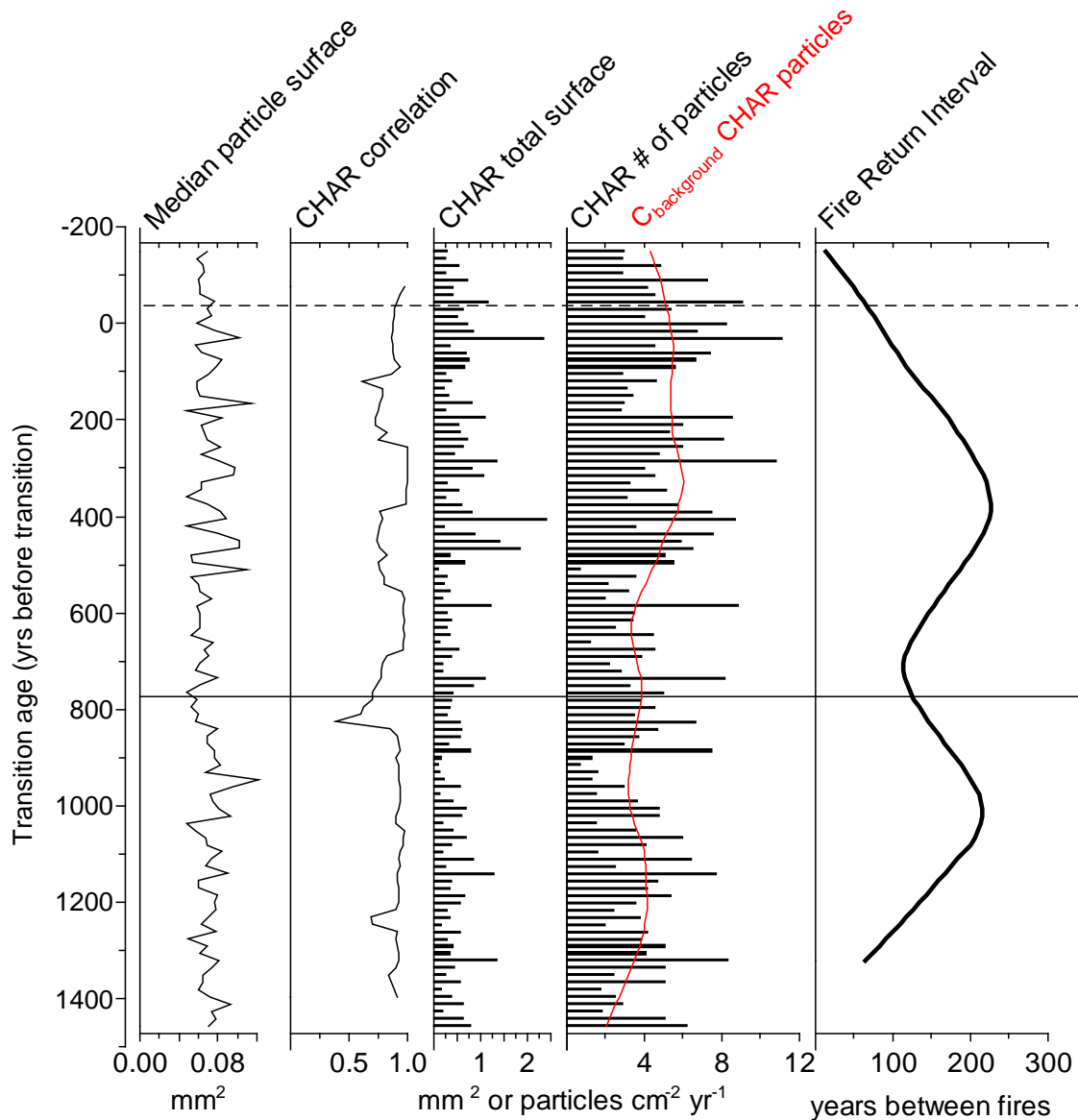


Figure 4: Chemical data comprising of: A) magnetic susceptibility of core AG004 11, B) grayscale, C) Calcium XRF counts, E) Titanium XRF counts, F) Silicon XRF counts, G) Si/Ti ratio XRF, H, I, J) LOI fluxes in  $g\ cm^{-2}\ yr^{-1}$ , K) Stacked LOI data indicating the dry weight percentages (% DW) of the constituents. The straight line indicates the pollen zonation and the dashed line the diatom zonation (see methods section).

### *Terrestrial and aquatic indicators - Macrocharcoal records*

As mentioned in the methods section, the Fire Return Interval (FRI) was calculated using a 400 year background smoothing and a 500 year FRI smoothing. In addition, the low frequency CHAR ( $C_{\text{background}}$ ) was estimated by using a Lowess smoother, while the high frequency CHAR ( $C_{\text{peak}}$ ) was estimated by residuals ( $\text{CHAR} - C_{\text{background}}$ ), a local threshold and a Gaussian mixture model. Based on the frequency and magnitude of  $C_{\text{peak}}$ , the FRI is inferred (figure 5). For example, when the frequency of peaks increases, the FRI decreases (e.g. from 300 yrs BT, figure 5). The charcoal background ( $C_{\text{background}}$ , figure 5) indicates a rather stable charcoal influx between 1500 and ~550 yrs BT followed by a period when charcoal influx was generally higher (~550 to -150 yrs BT).

The macrocharcoal median particle size (Figure 5) fluctuates around  $0.06 \text{ mm}^2$ . Maxima are around 950 yrs BT, between 500 and 400 yrs BT, around the 2<sup>nd</sup> turbidite (layer E, 308 yrs BT), 150 and 25 yrs BT. Macrocharcoal accumulation rates (CHAR) of either the number of particles or the total macrocharcoal surface per sample are also plotted in figure 5. A 10-point running correlation of the CHAR records (particle and surface) was also calculated (figure 5). There are several drops in the 10-pnt running correlation, but mostly there is a very good correlation (Pearson coefficient  $r > 0.75$ ). There are two prominent drops in the correlation, at 100 and 800 yrs BT. Also at around 250, 1250 yrs BT the correlation seems to decrease. The surface CHAR shows a few maxima, just before the transition, around 400, 1125 and 1325 yrs before the transition. The CHAR particle shows several increasing trends: from 1300-750 yrs BT, from 750-550 yrs BT, from 550-200 yrs BT and across the transition. The  $C_{\text{background}}$  of the CHAR particle is plotted to give an idea of the background (low frequency) accumulation. It increases from about  $3 \text{ particles cm}^{-2} \text{ yr}^{-1}$  to  $5 \text{ particles cm}^{-2} \text{ yr}^{-1}$  around 550 yrs BT. Finally the FRI (yrs between fire events) is displayed (figure 5). From the bottom upwards the FRI increases, with a maximum at 1005 yrs BT ( $\sim 215 \text{ yrs fire}^{-1}$ ), a minimum at 705 yrs BT ( $\sim 115 \text{ yrs fire}^{-1}$ ) and another maximum at 375 yrs BT ( $225 \text{ yrs fire}^{-1}$ ). From 375 yrs BT the FRI decreases to below  $25 \text{ yrs fire}^{-1}$ . The mean FRI was  $121 \text{ yrs fire}^{-1}$ .



**Figure 5: Macrocharcoal data consisting of: macrocharcoal median surface; CHAR 10-point running correlation; CHAR total surface accumulation; CHAR particle accumulation;  $C_{background}$  values of the CHAR particle; CHAR particle inferred FRI (see previous section for details). The straight line indicates the pollen zonation and the dashed line the diatom zonation (see methods section).**

*Terrestrial and aquatic indicators - Pollen-inferred vegetation dynamics*

In the percentage diagram (Figure 6) it is visible that overall vegetation changes little during the period analyzed. Using the Broken Stick model and Optimal partitioning the pollen record is split into two zones with a zone boundary at the midpoint between 765 and 780 yrs BT (~773 yrs BT). This zonation mainly coincides with an increase in *Quercus* and a decrease of *Corylus* pollen. Over the entire record, pollen assemblages are dominated by tree pollen (between 65% and 85% of the pollen sum). The pollen types with highest abundances among the tree pollen are *Quercus* and *Alnus* (~ 40% and ~ 20%, respectively), while pine (*Pinus*) and *Betula* are represented with lower values (~ 10%). Around 950 yrs BT there appears to be a maximum in fir (*Abies*). In the bottom part of the record (between 1000 and 1200 yrs BT) there is a decrease of tree pollen coinciding with an increase in shrub pollen. This is caused by the increase of hazel (*Corylus*) with a maximum at around 1150 yrs BT. At the bottom of the record *Pinus* temporarily increases to about 20%. Some pollen types have higher abundances at the bottom of the record (e.g. *Betula*, *Pinus*, *Artemisia*, *Plantago*), while others are more abundant at the right-hand of the diagram (*Juniperus* and *Fagus*). Between 1500 and 800 years BT, shrubs are more abundant together with a decrease in trees. The most prominent signal across the sediment colour transition is the gradual increase of *Fagus* pollen percentages. This pollen type is regularly recorded in pollen assemblages starting from ca. 350 yrs BT. The frequency of occurrences of *Juniperus* pollen increases towards the top of the section. The main components of the herbs are grasses (*Poaceae*, fluctuating around 5%), nettle (*Urtica*) and *Artemisia*, both fluctuating around 1%. Anthropogenic indicators (*Rumex* and *Urtica*) and ferns (*Pteridium*) occur irregularly in pollen assemblages. The final two graphs in figure 6 show the sample scores of the first principal component (PCA 1), which explains 15.9 % of the total variance, and the first detrended correspondence analysis (DCA 1). The PCA axis 1 sample scores are plotted in Figure 6.

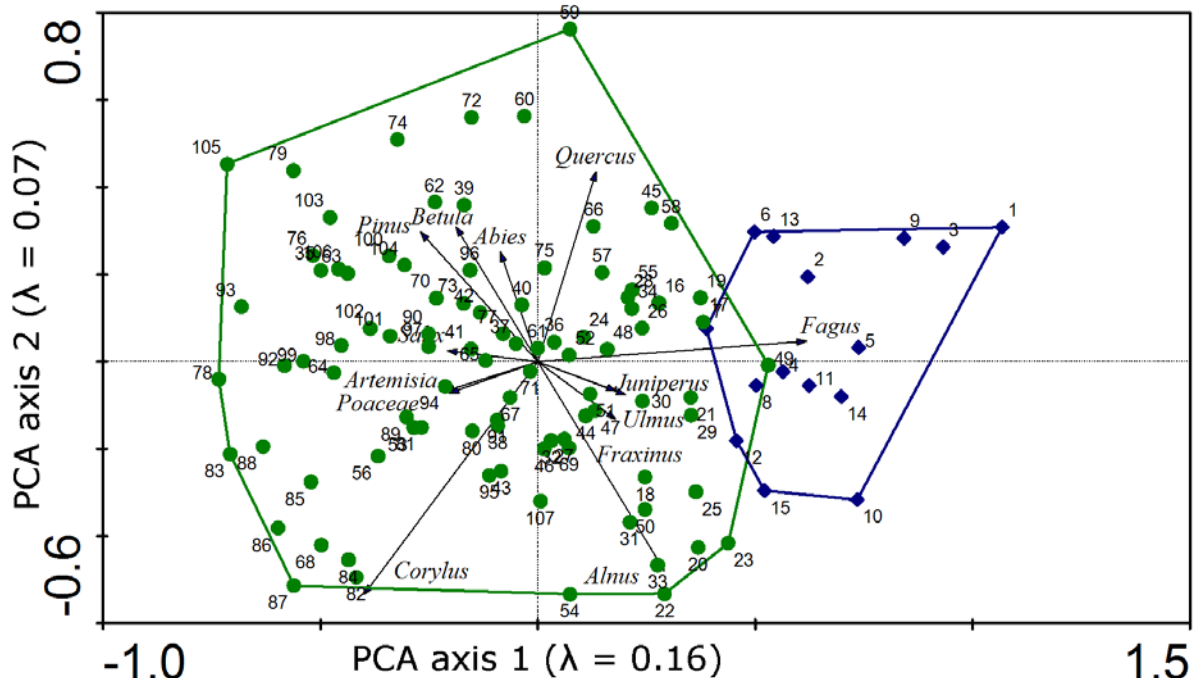


**Figure 7: Species and sample z-scores on the first two PCA axes, with indicated eigenvalues. Only species with a fit of at least 10% are shown, while all samples are shown. Samples are colour coded and grouped as: green- sample 1-15 (age -150 until 75 yrs BT) and blue- sample 16-108 (age 90 until 1455 yrs BT).**

Figure 7 shows that *Fagus* is almost perfectly positively correlated with the first axis, while more light demanding trees (*Pinus*, *Betula*, *Salix*), shrubs (*Corylus*) and herbs (*Poaceae* and *Artemisia*) are negatively correlated with the first axis. PCA axis 1 shows an increasing trend over time (Figure 6).

In the standardized pollen accumulation rate (PAR) diagram (Figure 8) the z-scores of selected pollen taxa are displayed in the same order as the sorted percentage diagram. Several peaks can be traced in almost each taxon, controlled by the total accumulation rate. When looking at the trees and shrubs, *Pinus* shows two distinct increases below the transition (at 1100-900 and 500-200 yrs BT) and it decreases above the transition. *Corylus* has high values around 1100 yrs BT, *Abies* has high values a few 100 years later, at 900 yrs BT. *Quercus*, *Alnus* and *Fraxinus* show increased PAR's from 700 till 100 yrs BT and again across the transition. *Ulmus*, *Juniperus* and *Fagus* show highest accumulation rates starting around 350 yrs BT. *Apiaceae*, *Artemisia* and *Poaceae* show high PAR's around 1100 yrs BT and between 500 and 400 yrs BT. *Urtica* and *Rumex* appear to have higher PAR's from about 900 yrs BT.

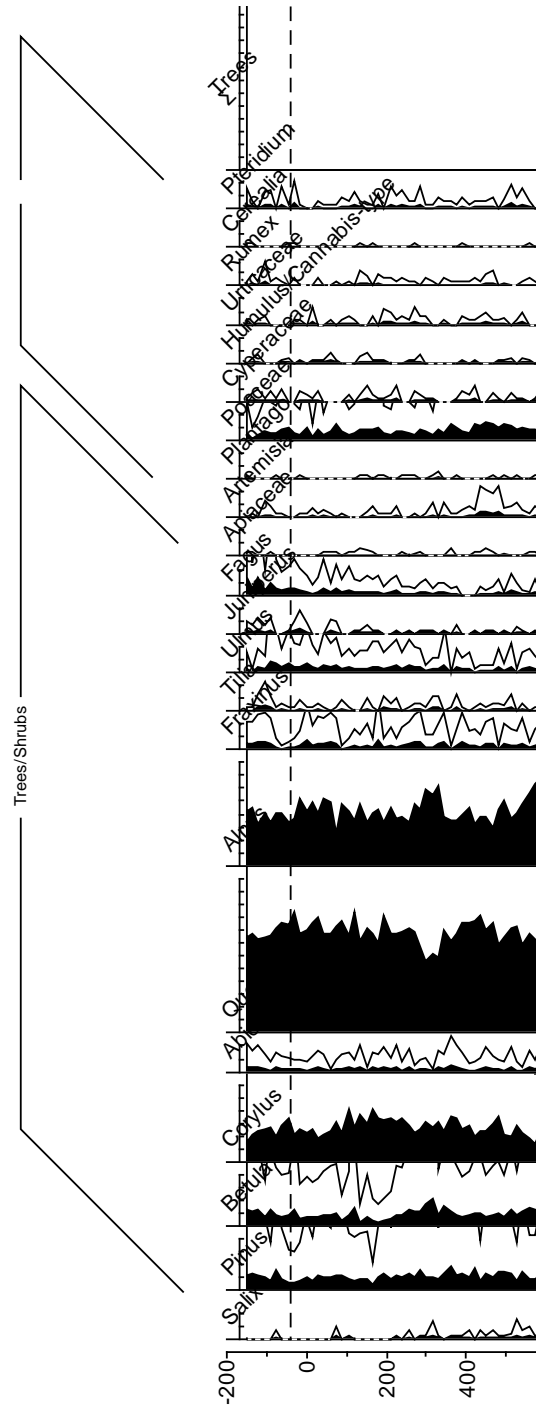
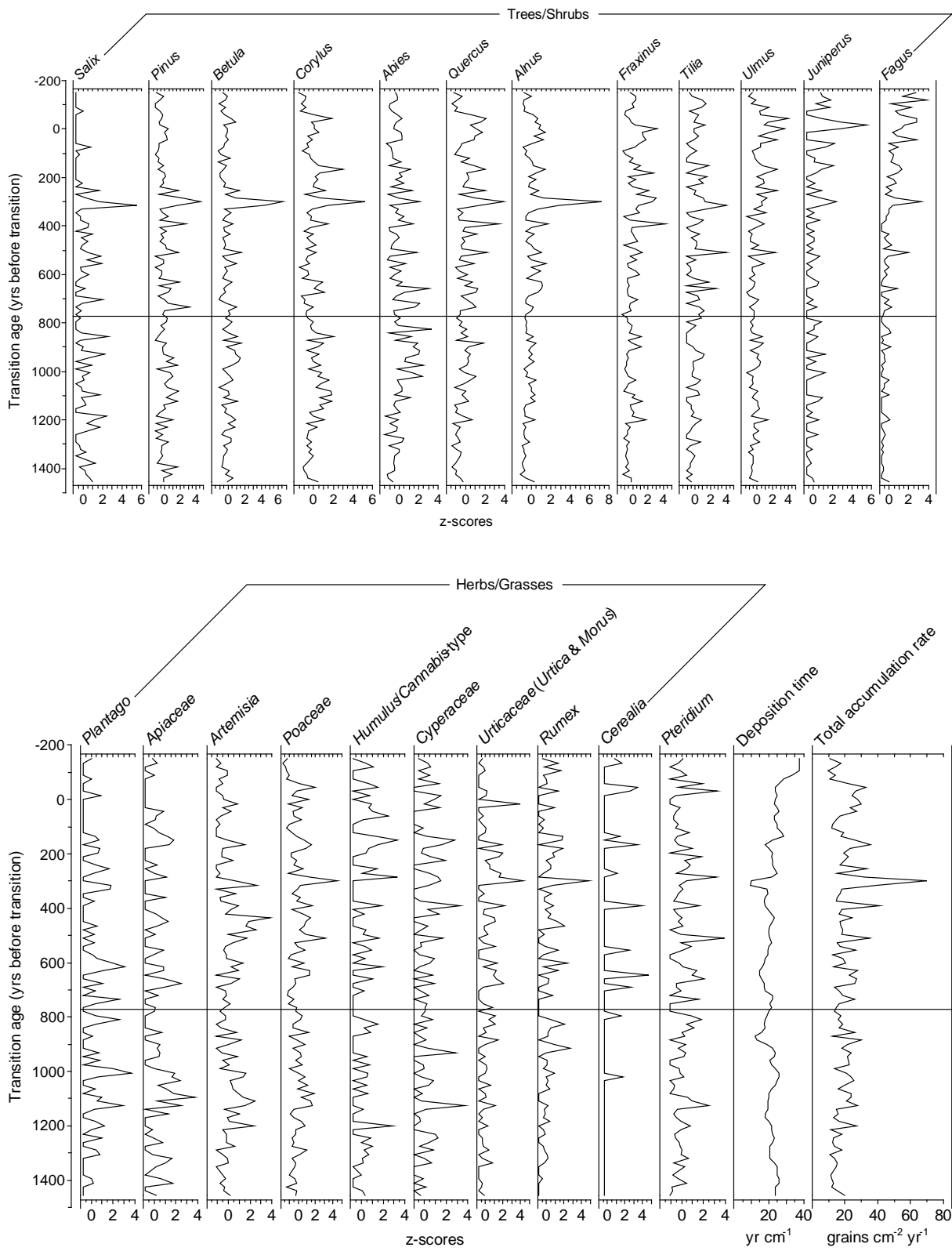


Figure 6: Pollen percentages of selected taxa from 5x exaggerated samples. The hollow curves are 5x exaggerated. Taxa sorted on percentage abundance from bottom left to top right. Afterwards the taxa were grouped as arboreal taxa, grasses/herbs and others. On the right are the stacked percentages of specific groups (excluding ferns and aquatic species). On the most right are the first axis of the PCA and DCA analysis of the pollen percentages. The dashed line indicates the diatom zonation, while the straight line indicates the pollen zonation (see methods section).



**Figure 8: AVG PAR standardized (z-scores) of selected taxa. The taxa were sorted based on percentages from bottom right to top left. The straight line indicates a pollen zone boundary (see Figure 6). The straight line indicates the pollen zonation (see methods section).**



### *Aquatic indicators - Diatom analyses*

The diatom record (Figure 9) was split into two significant zones (midpoint between -30 and -45 yrs BT). The assemblages show a stable dominance of planktonic species *Cyclotella* spp. (*C. comensis*, *C. distinguenda* var. *unipunctata*, and *C. ocellata*) stretching almost the entire length of the record until about -30 yrs BT. When comparing the individual contributions of the *Cyclotella* species, *C. distinguenda* var. *unipunctata* is the most dominant (~40-60% in most of the samples). *C. distinguenda* var. *unipunctata* shows a slowly decreasing trend from the bottom of the core up to 560 yrs BT. Thereafter *C. distinguenda* var. *unipunctata* increases from 545 yrs BT to 490 yrs BT. Between 490 yrs BT and -30 yrs BT there is a minimum around 180 yrs BT. Just prior to the youngest turbidite (~308 yrs BT) there is a decrease in planktonic species and an increase in *Fragilaria brevistriata* and *Fragilaria tenera* towards a combined total of about 15%. This disturbance lasts from about 30 years before the turbidite till about 30 years after, after which the planktonic diatom taxa are fully dominant (>95%) again. Just following the transition (-30 yrs BT) there is a rapid switch towards higher abundance of periphytic diatoms (e.g. *Amphora* sp., *Cymbella* sp., *Mastogloia* sp., and *Navicula* sp.) and *Fragilaria* spp. (*F. brevistriata* and *F. capucina* var. *vaucheria*). The planktonic AR fluctuates more or less the same as the total valve AR. The periphyton AR appears to be stable across the entire record, with fluctuations between 0.2 and 1.4 valves cm<sup>-2</sup> yr<sup>-1</sup>. Maxima can be seen near to the turbidites (at 795 and around 308 yrs BT). Prior to the oldest turbidite (~765 yrs BT) the *Fragilaria* AR increases from below 0.5\*10<sup>6</sup> to 2.2\*10<sup>6</sup> valves cm<sup>-2</sup> yr<sup>-1</sup>. The *Fragilaria* AR increases to 1.9\*10<sup>6</sup> valves cm<sup>-2</sup> yr<sup>-1</sup> around 315 yrs BT. The diatom inferred total phosphorus (DI-TP, R<sup>2</sup> 0.76; RMSEP 0.28; see methods section) appears to be relatively stable across most of the record, with a TP of around 12 µg l<sup>-1</sup> and a DI-TP reconstruction error between 1.92-2.03 µg l<sup>-1</sup>. With a lag of ~45 yrs after the transition, the DI-TP doubles (to ~24 µg l<sup>-1</sup>) over a time period of ~100 years.

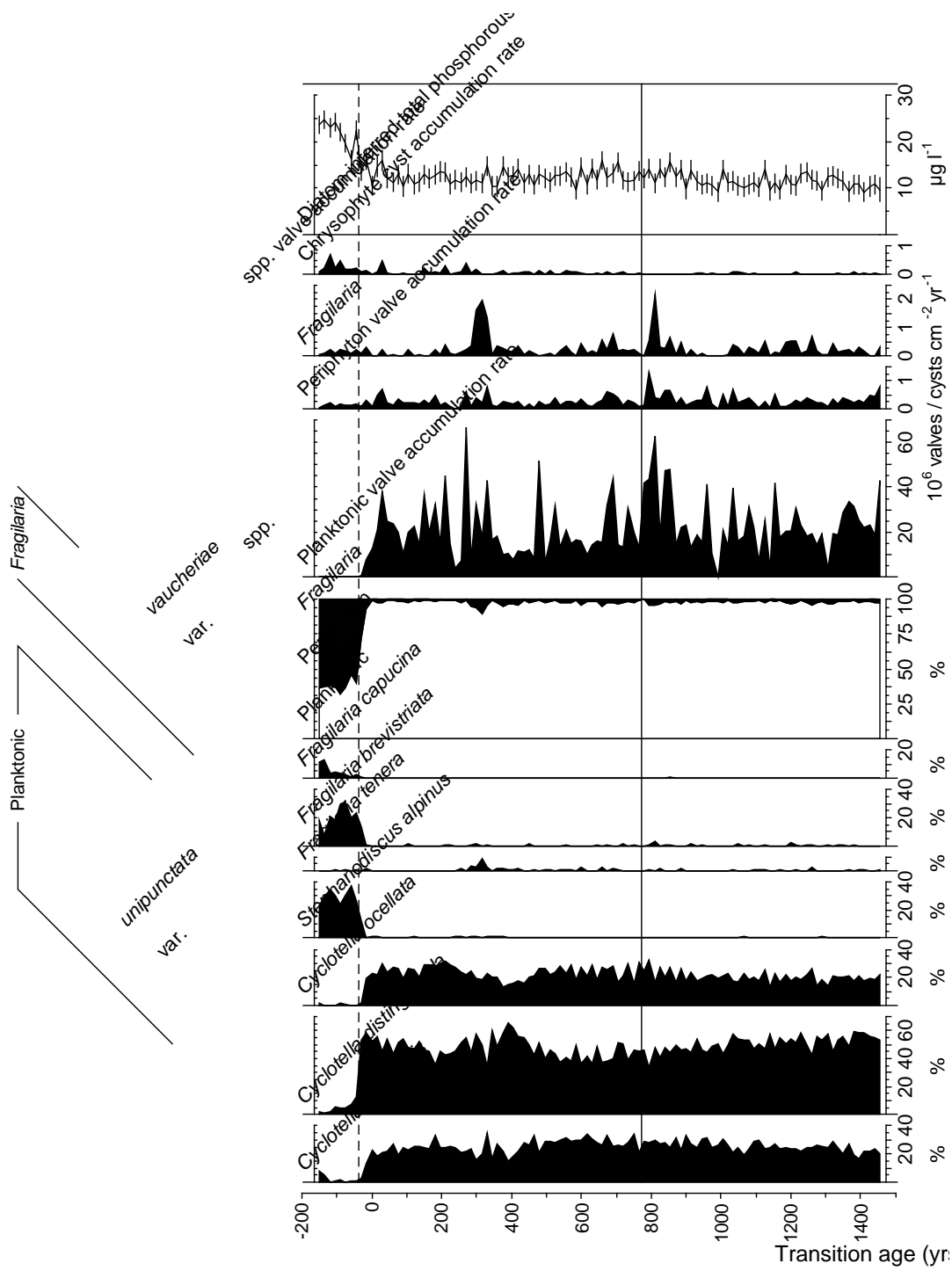
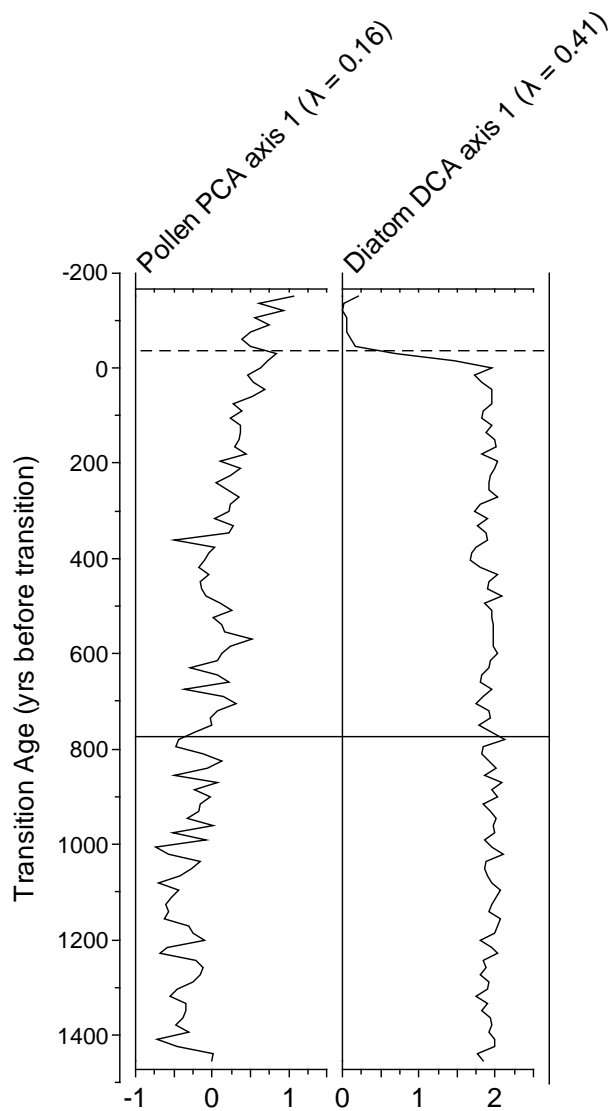


Figure 9: Diatom percentage abundance of selected taxa. The figures on the right are valve accumulation rates, both total as per group (planktonic, periphyton and *Fragilaria* spp. Using the EDDI combined TP dataset, a TP curve was reconstructed based on the species abundances of all taxa. The error bar is also given for the reconstructed TP. The straight line indicates the pollen zonation, while the dashed line indicates the diatom zonation (see methods section).

The figure below (figure 10) summarizes the observed changes in the vegetation and the diatom assemblages. The vegetation shows a steady increase on the first PCA axis, as mentioned in previous sections. The diatom assemblage 1<sup>st</sup> DCA axis appears steady up till the transition, when it drops dramatically within 30 years.



**Figure 10: Pollen 1<sup>st</sup> PCA axis and diatom 1<sup>st</sup> DCA axis. The straight line indicates the pollen zonation, while the dashed line indicates the diatom zonation.**

## Discussion

### *Physical and geochemical proxies*

The greyscale (an objective proxy of the sediment colour transition) shows a clear switch from bright to dark values at the top of the core (figure 4). From the oldest sample analysed (1455 yrs BT) up till about 550 yrs BT the greyscale is very similar to the XRF Calcium curve whereas from 550 yrs BT onwards the greyscale shows a trend more similar to the silica content (even though XRF Silicon is counted in 200x lower numbers). Around the turbidites (Layer E and G, 750 and 308 yrs BT respectively) there are increases in the erosional proxies (Ti, MS). Across the transition there is a similar increase, indicating higher erosion rates. Also it can be observed that the silica content shows a very similar change as the greyscale across the transition. The LOI organic matter percentage content shows an anti-relation with the greyscale (figure 4) in the years following the transition. However the LOI organic matter flux only shows a short term increase, indicating that increased organic matter percentages above the transition are actually driven by the reduction in silica. However there might be a short term increase in the organic matter flux. This indicates that actually the silica content is of dominant influence for the colour transition. The colour brightness over the entire record is likely to be a reflection of either the abundance of calcium carbonates or silica. Concerning the age scale, since the final varve counting was analyzed by one researcher, it can be assumed that if there is an error in the varve counting, this will be constant. The higher counting error during the pre-transition darker varves can be attributed to the thinner summer varve, indicating reduced summer mixing (e.g. O'Sullivan 1983; Antanoides 2007).

### *Terrestrial indicators - Vegetation dynamics*

From the pollen record it is apparent that overall vegetation was rather stable (figures 6, 7 and 8) for the period analyzed. This is comparable to the vegetation history of Lago Piccolo di Avigliana (Finsinger and Tinner 2006), in agreement with their largely overlapping pollen source area. Using the numerical zonation approach, the pollen record can be split into only two zones (with a statistically significant zone boundary at 773 yrs BT). Starting at Layer G (750 yrs BT) and more pronounced following Layer E (308 yrs BT) there is a reduction in *Abies* abundance, though since this species never reaches high percentages, it is difficult to validate whether this is a robust signal. *Corylus* is the dominant constituent to the shrubs sum, since the increase seen at 1150 and 850 yrs BT also shows a distinct increase in the shrubs sum in the stacked pollen figure (figure 7). Pollen assemblages are dominated by two pollen types (*Alnus* and *Quercus*) probably because there was a stable population of alder growing on the shores of the lake combined with an oak dominated forest in most of the catchment. *Pteridium*, which is often seen thriving following fire events, shows a more or less stable population across the record (Tinner et al. 2000; Finsinger et al. 2006). Since it is never present in percentages higher than 2%, it is difficult to interpret the response of this fire responsive fern. Finally, concerning human impact on the catchment, there is no evidence that human activities increased or decreased during the period analysed. Indicator species such as *Cerealia*, *Plantago*, *Rumex*, and *Urtica* (Behre 1981) show no distinct increase. Human presence in the catchment might be indicated by various settlements in the area prior, during and following the timeframe analyzed in this study, but it is unlikely that the vegetation was drastically altered by anthropogenic disturbance.

The PCA axis can be used to highlight the main vegetation changes. When looking at the sample scores of the first two PCA axes, it is apparent that the younger samples of the record (labelled: 1-15; -150 until 75 yrs BT) are grouped together, most dominantly on the 1<sup>st</sup> axis. This indicates that *Fagus*, which is almost perfectly correlated to this axis, is of major influence and that the *Fagus* expansion as observed in the pollen graphs is a major change in the vegetation. Secondly, since many of the more open-vegetation taxa (*Betula*, *Corylus*, *Plantago*, *Poaceae*, and *Artemisia*) are negatively correlated to the 1<sup>st</sup> axis, it might indicate that the vegetation is closing up by the *Fagus* cover. Furthermore, in the bottom part of the record (until 780 yrs BT) the 1<sup>st</sup> PCA axis shows overall lower values, indicating a more open vegetation. However pollen percentages generally underestimate shrubs and meadow abundances, as indicated by previous vegetation modelling studies (e.g. Sugita et al. 1999; Sugita 2007). This might indicate that the observed <5% fluctuations of shrubs and meadow species were actually more abundant. But care has to be taken as without a pollen productivity modelling study (e.g. Soepboer et al. 2008; Soepboer et al. 2010) this cannot be proven.

#### *Terrestrial indicators - Macrocharcoal-inferred fire regime*

Almost all peaks can be matched when comparing the CHAR surface and particle records (figure 5). This is confirmed by the running correlation CHAR. In agreement with previous studies (e.g. Tinner 2003; Ali et al. 2009) the macrocharcoal particle number and macrocharcoal total surface accumulation rates (CHAR<sub>n</sub> and CHAR<sub>s</sub> respectively) are highly and significantly correlated ( $r=0.972$ ,  $p<0.001$ ). By contrast, the median charcoal size and the CHAR records are not significantly correlated ( $p>0.1$ ). Difficulties lie with samples with a high total surface but containing many small charcoal particles as opposed to samples containing a few very large particles. Potentially the median particle size might be used to determine fire locality, as charcoal particle size is related to distance from the fire origin (Conedera et al. 2009). Several peaks can be traced in all three records (1425, 1320, 735, 465, 450, 405, 75 and 30 yrs BT) indicating a more local origin for these fire events. As indicated in the results section, the FRI was inferred from the macrocharcoal particle CHAR<sub>n</sub>. When peaks in the CHAR record are occurring more frequently (e.g. between 900 and 700 yrs BT) the FRI decreases. The lower FRI (thus higher fire-episode frequency) might also lead to opening of the forest and to increasing erosion rates all of which may increase nutrient supply to the lake (Kelly et al. 2006; Bradbury 1986). Interestingly the increase in the C<sub>background</sub> as inferred from CHAR<sub>n</sub> takes place around 550 yrs BT, while the main change in the pollen record is at ~772.5 yrs BT (figure 5). Even a minimum in the FRI occurs later than this pollen zonation, around 700 yrs BT. A shorter interval between fire episodes might lead to increased erosion and more frequent landslides, as indicated by a study on the effects of forest clearing by land-use change (Dapples et al. 2002). However it remains difficult to assess if this vegetation change can be linked to the fire regime, since only shore or local fires are generally detected in the pollen percentage record (Sugita et al. 1997). Around the transition the FRI shows a decreasing trend, together with an increase in *Fagus* pollen. Concerning the *Fagus* dynamics, see the next paragraph.

### *Terrestrial indicators - Fagus dynamics*

The most distinctly responding pollen taxon in the record is *Fagus*, which shows an increasing trend from about 225 yrs BT. This point can be interpreted as the rational limit (indicating the start of the population mass expansion), since from here on the pollen appear to occur continuously at >1% values (e.g. Watts 1973). The discontinuous presence of *Fagus* pollen and its low percentages (<1%) prior to the expansion indicate that a small population might have been present in the catchment for a longer period of time. Many studies have been published concerning the expansion of *Fagus sylvatica* (European beech; e.g. Tinner and Lotter 2006; Magri et al. 2006; Giesecke et al. 2007; Valsecchi et al. 2008). It is assumed that *Fagus* expanded from refugia in Croatia and Slovenia following the late Glacial/Younger Dryas. Based on genetic and pollen evidence, the expansion followed the mountain slopes, yet most of Northern Italy was not reached until around 5,000 cal. BP (Magri et al. 2006). In a review article (Tinner and Lotter 2006) the triggers behind the expansion of *Fagus* were discussed. Although the three study sites were located at somewhat higher altitudes (596-430 m a.s.l.) and latitudes (~47°N), the paper does give one of the most complete reviews concerning the subject. A heavily debated theory is that the species expanded naturally across southern Central Europe in response to climate change. The species prefers cooler and wetter climate and was potentially driven by short-term events. As demonstrated with the more thoroughly studied 8.2 kyr event, vegetation can respond very strongly to changing climatic conditions (e.g. Tinner and Lotter 2001).

Starting at the Bronze Age (roughly 4000 cal BP), when cultivation and forest clearing intensified in southern Central Europe (e.g. Valsecchi et al. 2006), the link between climatic change and *Fagus* expansion deteriorates (Tinner and Lotter 2006; Giesecke et al. 2007). Since the climatic conditions favoured *Fagus* expansion and fire was used to open forests and gain space for agriculture and pastures, the species could more easily expand, suggesting a combination of favourable conditions (Valsecchi 2008). However, it has been demonstrated that *Fagus* actually reacts negatively to human disturbances in Slovenia and Hungary (Gardner and Willis 1999). In the AVG catchment (this study) it is apparent that from 225 yrs BT *Fagus* increases, together with a reduction in the FRI. Since there is no clear evidence for a change in land use in the vegetation, it is difficult to interpret the *Fagus* expansion with respect to human impact. The theory that *Fagus* benefited from an increase in fire frequency might be plausible.

### *Aquatic indicators - Diatom dynamics*

The diatoms indicate a clear switch from planktonic species showing oligotrophic conditions towards benthic/littoral species indicating mesotrophic conditions, resulting in a doubling in the diatom inferred TP concentrations. A possible explanation for the DI-TP doubling is extended hypolimnic anoxia, which is a known cause for internal phosphorus loading (e.g. Boström et al. 1988; Antoniadou 2007). When looking at the diatom dynamics, it is striking that the increase in *Fragilaria* spp. is present around both a turbidite (Layer E, 308 yrs BT) and the post-transition sediment. *Fragilaria* spp. are indicators of lake disturbances, being capable of both benthic and planktonic life forms (Stockner and Benson 1967). A link between short term weather conditions and *Cyclotella* and *Fragilaria* dynamics has been observed in a previous study (Tolotti et al. 2007). This indicated that *Cyclotella* flourishes under stable oligotrophic conditions, while *Fragilaria* responds favourably to environmental variability such as changes in oxygen supply and nutrient levels. Furthermore small benthic *Fragilaria* taxa are often expanding shortly following deglaciation in North America (Smol and Boucherle 1985). When looking at the accumulation rates, it can be determined that the periphyton and *Fragilaria* AR appear more or less stable over the entire record (except for turbidite excursions), while the planktonic AR shows a massive reduction following the transition. This is reflected in the species percentages, since although it appears that the periphyton is increasing, it is more significantly the planktonic species that are actually decreasing. Since *Cyclotella* species have a more delicate frustule than for instance *Stephanodiscus* species, dissolution by changing pH might be possible. To check for changing pH, a pH reconstruction was performed. Although the RMSEP of the reconstruction was high ( $r^2$ : 0.83; RMSEP: 0.39), it indicated that the pH fluctuated irregularly between 6.2 and 9.6, indicating slightly acidic to alkaline conditions, respectively. Silica tends to dissolve under high pH (pH>9, e.g. Levin 1960, Barker et al. 1994) thus during most of the record the pH would not have had an influence on silica levels. However care has to be taken as these pH reconstructions are not designed for alkaline carbonate rich lakes, such as AVG. Another cause for the reduction in silica might be that following the eutrophication, production rose to such level that silica became a limiting nutrient. Evidence for a short term increase in production following the transition can be seen in the LOI Org. Mat. flux (figure 4). Subsequent years of high production and decreased silica influx could lead to observed depletion of silica. This might explain the 30 year lag of the diatom response to the colour transition. Studies on the Great Lakes in Canada (e.g. Schelske et al. 1983; Conley and Schelske 2001) have shown that even a relatively small increase in TP (~10  $\mu\text{g l}^{-1}$ ) might increase production to such a level that silica becomes limiting. Although the oligotrophic Canadian lakes might be more sensitive to this, the silica to phosphorous ratio most likely has decreased, allowing non-siliceous organisms to become more dominant (Tilman 1989). *Stephanodiscus* spp. are also known for their adaptation to low Si:P ratios (Kilham et al. 1986; Kilham et al. 1996). Finally lowering of the water level might lead to an increase of periphytic species, as would explain the increase in chrysophytes, since epiphytic chrysophytes increase with macrophytes.

*Comparison Lago Grande di Avigliana: Copper Age and the last ~200 years*

A study on AVG (Finsinger et al 2006) was performed on the vegetation in the catchment and the diatom assemblages, derived from lake sediment dated to 1830-2000 yrs AD.

The vegetation during the pre-industrial and recent periods was very different from the Copper Age vegetation, primarily due to human cultivation activities. Therefore they are difficult to compare. Furthermore since the Bronze Age several plant species have been cultivated (e.g. *Cerealia*, *Castanea* and *Juglans*) causing a distinct change by human impact apparent in the pollen curves.

The diatom assemblages are however quite comparable. These indicate stable mesotrophic conditions ( $<25 \mu\text{g l}^{-1}$ ) from 1830- 1950 yrs AD. The species composition is very similar for the period analyzed during the Copper Age, with the dominant planktonic species was the same as during the Copper Age (*Cyclotella distinguenda* var.

*unipunctata*, mentioned as *C. cyclopuncta*). Sewage discharge from the city of Avigliana added a lot of nutrients to into the lake and it became eutrophied from about 1950. This led to a dominance of *Stephanodiscus*, *Cyclostephanus* and *Fragilaria* species. This is reflected in the DI-TP, which indicates highly eutrophic conditions ( $>100 \mu\text{g l}^{-1}$ ) from 1965 until 1980. Due to drainage deflections the DI-TP has decreased considerable to  $40 \mu\text{g l}^{-1}$ . This is still considerable higher than the previously measured mesotrophic conditions ( $<25 \mu\text{g l}^{-1}$ ). Species dominant during the oligotrophic pre-transition Copper Age period are also dominant during the 19<sup>th</sup> and early 20<sup>th</sup> century. This might indicate that the Si:P ratio was actually quite similar when comparing the pre-transition Copper Age and the 19<sup>th</sup> to early 20<sup>th</sup> century. Furthermore the recent eutrophication (1965-1980 yrs AD) leads to a similar species response as observed following the Copper Age silica depletion. This indicates that both a phosphor increase and a silica decrease leads to a similar response concerning *Stephanodiscus* species dominance replacing *Cyclotella* species.



### *Sediment runoff dynamics and influence on lake ecosystems*

In the geochemistry are several factors indicating increased erosion, potentially driven by wetter conditions. There is a significant increase in magnetic susceptibility and a weaker increase in Ti and Fe (figure 4). These increases can also be seen around the turbidites (layers E and G, 750 and 308 yrs BT respectively). This indicates that erosion might have increased during the transition. Another effect of large fire events is the potential influence on erosion fluxes and therefore nutrient supply (Bradbury 1986; Kelly et al. 2006). Opening of the vegetation is a potential consequence of large fire events. This might lead to increased erosion and more frequent landslides, as indicated by a study on landscape changes (Dapples et al. 2002). However a running correlation between charcoal proxies and Ti fluctuated heavily between negative and positive values, indicating that another factor controlled these variables (data not shown). In the pollen record from AVG (Figures 7 and 9) it is difficult to discern distinct changes in vegetation composition. The large size of the lake certainly makes it difficult to detect a vegetation response to individual fire events. In fact, the pollen source area of this 0.83 km<sup>2</sup> lake is large (in the order of 10 km<sup>2</sup>, table 1), and likely larger than the size of the disturbance by fire events. Thus overall the vegetation composition appears more or less stable for the largest part of the record, with the notable exception of a *Fagus* increase. Since the vegetation does not appear to change to a more open vegetation (for instance with more dominant shrubs or herbs) it is unlikely that there was a drastic increase in fire driven erosion leading to the sediment colour transition. The largest changes in the geochemical proxies occurred in Silica content (see previous sections). The observed increase in the MS at the top of the record (starting at ~210 yrs BT) erosion might have another cause. Diagenesis can increase magnetic compounds in the sediment (Sandgren and Snowball 2001; Butler 2004), specifically the Fe abundance. Furthermore the terrestrial fraction (containing magnetic components) is likely higher due to the silica depletion (Peck et al. 1994). Further information about climate controlled precipitation might be found in lake level reconstructions. Lake levels have been reconstructed in both central Europe (Magny 2004) and central Italy (Magny et al. 2007), reflecting climatic changes. Lake levels may be reconstructed by a sedimentological approach, based on markers in the lithology and macroscopic components in lake marl (for further details e.g. Magny 2006). In both central Europe and Central Italy a lake-level high stand was found at around 4800 cal yrs BP, followed by lake-level low stand (Figure 11). After these oscillations the lake levels steadily increased with distinct minima intermittent, to its present high lake level. Thus a climatic trigger is a potential driving factor for the sediment transition.

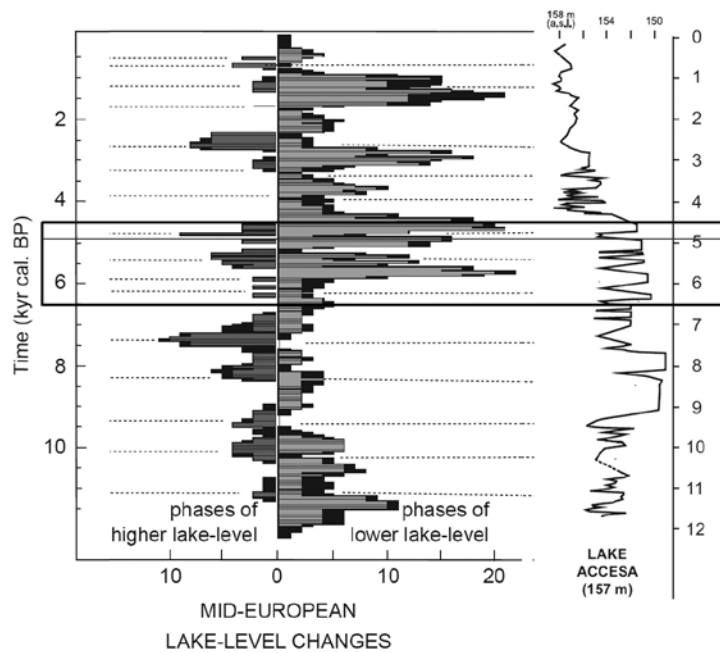


**Figure 11: Reconstructed lake level changes. The horizontal axis in the figure on the left indicates the amount of successive 50yr lake levels. In the figure on the right the actual lake level was reconstructed. Age in calibrated years BP, adapted from Magny 2004 and Magny et al. 2007. The black box covers 6500-4500 cal yrs BP, where the interval analyzed in this study should fall within.**

#### *Lake level fluctuations and climate change*

As discussed earlier, several proxies (XRF Silicon, Si/Ti ratio, macrocharcoal proxies, and diatom assemblages) indicate a cool and dry period. Interestingly, the lake level studies indicate a lake level high stand during and following the transition (thin horizontal line in Figure 11). The lake-level change inferred increase in precipitation is potentially reflected by the maximum in the FRI around 400 yrs BT (figure 5). Thus the consequent reduction in the FRI would agree with the consequent reduction in lake level, in line with a previous study of lake levels and fire events (Hallet et al. 2003). The low lake level, as can be seen starting around 4700 cal. yrs BP (Magny 2004; Magny et al. 2007; Figure 11) could thus be a likely trigger for the sediment colour transition. Further evidence of climatic instability comes from a study focussing on Holocene climate variability in central Europe (Haas et al. 1998), where a cool and wet interval has been observed from 4600-4400 cal yrs BP.

## Conclusions

The factor controlling the observed sediment colour change is the silica reduction, primarily caused by a massive reduction in planktonic species valve AR. As for the cause of this eutrophication, human impact can be ruled out as few anthropogenic indicators were found in the vegetation. However a climatic cause can be one of two opposites. Wetter conditions (as indicated by the *Fagus* expansion) might have led to increased erosion. This is confirmed by the erosional proxies (MS and XRF Ti, Fe). As more nutrient rich topsoil is washed into the lake, eutrophication is often the consequence (e.g. Lal 1976). However the shift found in the erosional proxies can just as likely be explained by the dramatic reduction in silica.

Pollen zonation indicates that the major change in the vegetation occurred prior to the increase in background charcoal accumulation, though at a similar time as a minimum in the FRI (~700 yrs BT, figure 5). This hints that changes in the vegetation are actually leading changes in macrocharcoal. However there are also several proxies which indicate dryer conditions (macrocharcoal, Chrysophytes and diatom assemblages). An explanation might be that cooler conditions have led to extended ice cover, combined with a weakening of the summer melt-water influx. This caused stratification to remain for a longer period. A reduction in lake level would lead to a higher nutrient concentration. Furthermore bottom water anoxia might lead to phosphor release, as might be derived from the increased iron content following the transition. As the meltwater flux decreases, the silica influx will also decrease, leading to a silica limited system, as observed by the collapse of planktonic diatom accumulation (figure 9). Dryer conditions have been theorized as a mechanism resulting in a low Si:P ratio (Kilham et al. 1996). Longer winter conditions are also an explanation for the observed increase in *Stephanodiscus* spp. and chrysophyte cysts, as these are most abundant during winter months (Heron 1961).

Concerning the speed with which the ecosystem changes, this differs between the terrestrial and aquatic realm (also visible in figure 10). The vegetation appears to be more or less stable, as indicated by the macrocharcoal and pollen data. The observed rate of change in the terrestrial realm is relatively slow, gradually changing over several centennials. This is slower than the observed rate of change during more intense climatic changes, such as the 8.2 ka event (Tinner and Lotter 2001). In the AVG catchment it is likely that the standing vegetation was largely able to cope with the Copper Age climatic change. This is in opposition to the aquatic ecosystem, as the diatom and lake chemistry appear to change within 30 years. The DI-TP appears to increase more gradual, doubling over ~100 years. The rapidity with which lake ecosystems can change is comparable to studies on recent lake sediments (Lotter et al. 1997; Finsinger et al. 2006), which indicate a decadal response time. The key difference between these studies is anthropogenic disturbance versus climatic disturbance. Thus this study indicates that climatic disturbance can trigger a change in lake-ecosystems at a similar speed as recent anthropogenic disturbances.

## Literature

- Ali, A. A., Higuera, P. E., Bergeron, Y., Carcaillet, C. 2009. Comparing fire-history interpretations based on area, number and estimated volume of macroscopic charcoal in lake sediments. *Quaternary Research*, 72, p.462-468.
- Ammann, B., Birks, H. J. B., Brooks, S. J., Eicher, U., von Grafenstein, U., Hofmann, W., Lemdahl, G., Schwander, J., Tobolski, K., Wick, L. 2000. Quantification of biotic responses to rapid climatic changes around the Younger Dryas - a synthesis. *Palaeogeography Palaeoclimatology Palaeoecology*, 159, p.313-347.
- Antoniades, D. 2007. Lake Chemistry. In Elias, S.A., editor, *Encyclopedia of Quaternary Science*. Elsevier, p.2038-2046.
- Behre, K. E. 1981. The interpretation of anthropogenic indicators in pollen diagrams. *Pollen et Spores* 23, p.225-245.
- Beug, H.-J. 2004. Leitfaden der Pollenbestimmung für Mitteleuropa und angrenzende Gebiete. Verlag Dr. Friedrich Pfeil, 542p.
- Biancotti, A., Bellardone, G. S. B., Cagnazzi, B., Giacomelli, L., Marchisio, C. 1998. Regional distribution of rainfalls and temperatures. *Climatological Studies in Piedmont*, 1, p.1-80.
- Birks, H. J. B., Berglund, B.E. 1979. Holocene pollen stratigraphy of southern Sweden: a reappraisal using numerical methods. *Boreas* 8, p.257-279.
- Birks, H. J. B. 1986. Numerical zonation, comparison and correlation of Quaternary pollen-stratigraphical data. In Berglund, B. E., editor, *Handbook of Holocene Palaeoecology and Palaeohydrology*, John Wiley & Sons, Chichester, p.743-774.
- Boström, B., Andersen, J. M., Fleischer, S., Jansson, M. 1988. Exchange of phosphorus across the sediment-water interface. *Hydrobiologia* 170, p.229-244
- Bradbury, J. P. 1986. Effects of forest fire and other disturbances on wilderness lakes in northeastern Minnesota II. *Archiv für Hydrobiologie*. Stuttgart [Arch. Hydrobiol.]. Vol. 106, no. 2, p.203-217.
- Brown, E. T., Johnson, T. C., Scholz, C. A., Cohen, A. S., King, J. W. 2007. Abrupt change in tropical African climate linked to the bipolar seesaw over the past 55,000 years. *Geophys. Res. Lett.*, 34, L20702.
- Butler, R. F. 2004. *Paleomagnetism: Magnetic Domains to Geologic Terranes*. 248 pp. permanent link: [http://geography.lancs.ac.uk/cemp/resources/Butler\\_book/contents.htm](http://geography.lancs.ac.uk/cemp/resources/Butler_book/contents.htm)
- Carcaillet, C. 2007. Charred Particle Analysis. In Elias, S.A., editor, *Encyclopedia of Quaternary Science*. Elsevier, p.1582-1593.
- Carcaillet, C., Bouvier, M., Fréchette, B., Larouche, A. C., Richard, P. J. H. 2001. Comparison of pollen-slide and sieving methods in lacustrine charcoal analyses for local and regional fire history. *The Holocene*, 11, p.467-476.
- Clark, J. S. 1990. Fire and climate change during the last 750 yr in northwestern Minnesota. *Ecological Monographs* 60, p.135-159.
- Colombaroli, D., Marchetto, A., Tinner, W. 2007. Long-term interactions between Mediterranean climate, vegetation and fire regime at Lago di Massaciuccoli (Tuscany, Italy). *Journal of Ecology*, 95, p.755-770.

- Conedera, M., Tinner, W., Neff, C., Meurer, M., Dickens, A. F., Krebs, P. 2009. Reconstructing past fire regimes: methods, applications, and relevance to fire management and conservation. *Quaternary Science Reviews* 28, p.555–576.
- Conley, D. J., Schelske, C. L. 2001. Biogenic silica, p. 281–293. In eds Smol, J. P., Birks, H. J. B., Last, W. M., *Tracking environmental changes in lake sediments. V. 3: Terrestrial, algal, and siliceous indicators.* Kluwer.
- Croudace, I. W., Rindby, A., Rothwell, R. G. 2006. ITRAX: description and evaluation of a new multi-function X-ray core scanner. *Geological Society, London, Special Publications* v. 267, p.51-63.
- Dapples, F., Lotter, A. F., van Leeuwen, J. F. N., van der Knaap, W. O., Dimitriadis, S., Oswald, D. 2002. Paleolimnological evidence for increased landslide activity due to forest clearing and land-use since 3600 cal BP in the western Swiss Alps. *Journal of Paleolimnology*, 27, p.239-248.
- Dearing, J. A., Battarbee, R. W., Dikau, R., Larocque, I., Oldfield, F. 2006. Human–environment interactions: towards synthesis and simulation. *Reg Environ Change*, 6, p.115–123.
- Ellenberg, H. 1996. *Vegetation Mitteleuropas mit den Alpen in ökologischer, dynamischer und historischer Sicht.*, Eugen Ulmer, Stuttgart, 1096 pp.
- Finsinger, W. and Tinner, W. 2006. Holocene vegetation and land-use changes in response to climatic changes in the forelands of the southwestern Alps, Italy. *Journal of Quaternary Science*, 21(3), p.243-258.
- Finsinger, W., Bigler, C., Krähenbühl, U., Lotter, A. F., Ammann, B. 2006. Human impacts and eutrophication patterns during the past ~200 years at Lago Grande di Avigliana (N. Italy). *J Paleolimnol*, 36, p.55-67.
- Gaggino G, Cappelletti E, Marchetti R, Calcagnini T (1985) La qualità delle acque dei laghi Italiani negli anni '80, Inquinamento e recupero dei laghi. Atti del Congresso Internazionale European water Pollution Control Association, ANDIS, Associazione Nazionale di Ingegneria Sanitaria, Roma, p.5–32
- Gardner, A. R., Willis, K. J. 1999. Prehistoric farming and the postglacial expansion of beech and hombeam: a comment on Küster. *The Holocene*, 9(1), p.119-122.
- Giesecke, T., Hickler, T., Kunkel, T., Sykes, M. T., Bradshaw, R. H. W. 2007. Towards an understanding of the Holocene distribution of *Fagus sylvatica* L. *J. Biogeogr.*, 34, p.118-131.
- Grimm, E.C. 1991–2004. TILIA, TILA.GRAPH, and TGView. Illinois State Museum, Research and Collections Center, Spring-field, USA (<http://demeter.museum.state.il.us/pub /grimm/>)
- Haas, J. N., Richoz, I., Tinner, W., Wick, W. 1998. Synchronous Holocene climatic oscillations recorded on the Swiss Plateau and at timberline in the Alps *The Holocene* (May), 8(3), p.301-309.
- Hallet, D. J., Mathewes, R. W., Walker, R. C. 2003. A 1000-year record of forest fire, drought and lake-level change in southeastern British Columbia, Canada. *The Holocene* 13, p.751-761

Heiri, O., Lotter, A. F., Lemcke, G. 2001. Loss on ignition as a method for estimating organic and carbonate content in sediments: reproducibility and comparability of results. *Journal of Paleolimnology*, 25, p.101-110.

Heron, J. 1961. The Seasonal Variation of Phosphate, Silicate, and Nitrate in Waters of the English Lake District. *Limn. Ocean.*, Vol. 6, No. 3 (July), p.338-346.

Higuera, P. E., Brubaker, L. B., Anderson, P. M., Brown, T. A., Kennedy, A. T., Hu, F. S. 2008. Frequent Fires in Ancient Shrub Tundra: Implications of Paleorecords for Arctic Environmental Change. *PLoS ONE*, 3(3), e00017744.

Hofmann C., Conedera, M., Delarze R., Carraro, G. and Giorgetti, P. 1998: Effets des incendies de forêt sur la végétation au Sud des Alpes suisses. *Mitteilungen der Eidgenössischen Forschungsanstalt für Wald, Schnee und Landschaft* 73, p.1–90.

Juggins, S. 2007. C2 Version 1.5 User guide. Software for ecological and palaeoecological data analysis and visualization. Newcastle University.

Kelly, E. N., Schindler, D. W., St. Louis, V. L., Donald, D. B., Vladicka, K. E. 2006. Forest Fire Increases Mercury Accumulation by Fishes via Food Web Restructuring and Increased Mercury Inputs. *PNAS*, Vol. 103, No. 51 (Dec. 19), p.19380-19385.

Kilham, P., Kilham, S. S., Hecky, R. E. 1986. Hypothesized Resource Relationships Among African Planktonic Diatoms. *Limnology and Oceanography*, Vol. 31, No. 6, p. 1169-1181

Kilham, S. S., Theriot, E. C., Fritz, S. C. 1996. Linking Planktonic Diatoms and Climate Change in the Large Lakes of the Yellowstone Ecosystem Using Resource Theory. *Limn. Ocean.*, Vol. 41, No. 5, *Freshwater Ecosystems and Climate Change in North America* (July), p.1052-1062.

Krammer, K., Lange-Bertalot, H. 1991. Bacillariophyceae 4. Teil: Achnantheaceae. In: H. Ettl, G. Gärtner, J. Gerloff, H. Heynig, D. Mollenhauer (eds.), *Süßwasserflora von Mitteleuropa*, Band 2/4. Gustav Fischer Verlag, Heidelberg, 437pp.

Krammer, K., Lange-Bertalot, H. 1999a. Bacillariophyceae 1. Teil: Naviculaceae. In: H. Ettl, J. Gerloff, H. Heynig, D. Mollenhauer (eds.), *Süßwasserflora von Mitteleuropa*, Band 2/1. Gustav Fischer Verlag, Heidelberg, 876 pp.

Krammer, K., Lange-Bertalot, H. 1999b. Bacillariophyceae 2. Teil: Bacillariaceae, Epithemiaceae, Surirellaceae. In: H. Ettl, J. Gerloff, H. Heynig, D. Mollenhauer (eds.), *Süßwasserflora von Mitteleuropa*, Band 2/2. Gustav Fischer Verlag, Heidelberg, 611pp.

Krammer, K., Lange-Bertalot, H. 2000. Bacillariophyceae 3. Teil: Centrales, Fragilariaceae, Eunotiaceae. In: H. Ettl, G. Gärtner, J. Gerloff, H. Heynig & D. Mollenhauer (ed.), *Süßwasserflora von Mitteleuropa*, Band 2/3. Gustav Fischer Verlag, Heidelberg, 599pp.

Lal, R., 1976. Soil erosion on Alfisols in Western Nigeria, IV. Nutrient element losses in runoff and eroded sediments. *Geoderma*, 16, p.403--417

Lamoureux, S. F., Bradley, R. S. 1996. A late Holocene varved sediment record of environmental change from northern Ellesmere Island, Canada. *Journal of Paleolimnology* 16, p.239-255.

Lewin, J. C. 1960. The dissolution of silica from diatom walls. *Geochimica et Cosmochimica Acta*, Vol. 21, p.182-198.

- Lotter, A. F. 1988. Paläoökologische und Paläolimnologische Studie des Rotsees bei Luzern. PhD thesis, Universität Bern, Bern.
- Lotter, A. F. 1989. Evidence of annual layering in Holocene sediments of Soppensee, Switzerland. *Aquatic Sciences*, 51(1), p.19-30.
- Lotter, A.F., Juggins, S. 1991. POLPROF, TRAN and ZONE. Programs for plotting, editing and zoning pollen and diatom data. INQUA Commission for the study of the Holocene, Working Group on Data Handling Methods, Newsletter 6.  
(<http://www.staff.ncl.ac.uk/staff/stephen.juggins/software.htm>)
- Lotter, A. F., Birks, H. J. B. 1997. The separation of the influence of nutrients and climate on the varve time-series of Baldeggersee, Switzerland. *Aquatic Sciences*, Vol. 59, p.362-375.
- Lotter, A. F., Sturm, M., Teranes, J. L., Wehrli, B. 1997. Varve formation since 1885 and high-resolution varve analyses in hypertrophic Baldeggersee (Switzerland). *Aquat Sci* 59, p.304–325.
- Magny, M. 2004. Holocene climate variability as reflected by mid-European lake-level fluctuations and its probable impact on prehistoric human settlements. *Quaternary International*, 113, p.65-79.
- Magny, M. 2006. Holocene fluctuations of lake levels in west-central Europe: methods of reconstruction, regional pattern, palaeoclimatic significance and forcing factors. In Elias, S. A., editor, *Encyclopaedia of Quaternary geology*. *Encyclopaedia of Quaternary Science*, Elsevier, p.1389-1399.
- Magny, M., de Beaulieu, J-L., Drescher-Schneider, R., Vannièrè, B., Walter-Simonnet, A-V., Miras, Y., Millet, L., Bossuet, G., Peyron, O., Brugiapaglia, E., Leroux, A. 2007. Holocene climate changes in the central Mediterranean as recorded by lake-level fluctuations at Lake Accesa (Tuscany, Italy). *Quaternary Science Reviews*, 26, p.1736-1758.
- Magri, D., Vendramin, G. G., Comps, B., Dupanloup, I., Geburek, T., Gömöry, D., Latalowa, M., Litt, T., Paule, L., R., J. M., Tantau, I., van der Knaap, W. O., Petit, R. J., de Beaulieu, J-L. 2006. A new scenario for the Quaternary history of European beech populations: palaeobotanical evidence and genetic consequences. *New Phytologist*, 171, p.199-221.
- Maher, L. J. 1972 Nomograms for Computing 0.95 Confidence Limits of Pollen Data. *Rev. Palaeobot. Palynol.*, 13, p.85-93.
- Mayewski, P. A., Rohling, E., E., Stager, J., C., Karlen, W., Maasch, K., A., Meeker, L., D., Meyerson, E., A., Gasse, F., van Kreveld, S., Holmgren, K., Lee-Thorp, J., Rosqvist, G., Rack, F., Staubwasser, M., Schneider, R., R., Steig, E., J. 2004 Holocene climate variability. *Quaternary Research*, Volume 62, Issue 3, November, p.243-255.
- Messerli, B., Grosjean, M., Hofer, T., Núñez, L., Pfister, C. 2000 From nature-dominated to human-dominated environmental changes. *Q Sci Rev*, 19, p.459–479.
- Moore, P. D., Webb, J.A., Collinson, M.E. 1991. *Pollen Analysis* (2nd edn). Blackwell Scientific Publications: Oxford. 216p.
- Moser, K. A., Smol, J. P., MacDonald, G. M., Larsen, C. P. S. 2002. 19th century eutrophication of a remote boreal lake: a consequence of climate warming? *Journal of Paleolimnology* 28, p.269-281.

Nowaczyk 2001 . Logging of Magnetic Susceptibility. In Last, W.M., Smol, J.P. editors, Tracking Environmental Change Using Lake Sediments, vol. 1, Kluwer Academic Publishers, Dordrecht, p.155-170.

O'Sullivan, P. E. 1983. Annually-Laminated lake sediments and the study of Quaternary environmental changes – A Review. Quaternary Science Reviews, Vol. 1, p.245-313.

Peck, J. A., King, J. W., Colman, S. M., Kravchinsky, V. A. 1994. A rock-magnetic record from Lake Baikal, Siberia: Evidence for Late Quaternary climate change. Earth and Planetary Science Letters 122, p.221-238

Pessina, A. 2000. Il primo neolitico dell'Italia settentrionale. Problemi generali. In: Pessina A, Muscio G (eds.) La neolitizzazione tra oriente e occidente. Atti del Convegno di Studi. Udine, 23-24 aprile 1999, Comune di Udine. Edizioni del Museo Friulano di Storia Naturale, Udine, p.81-90.

Petrucci, F., Bortolami, G. C., Dal Piaz, G. V. 1970. Ricerche sull'anfiteatro morenico di Rivoli-Avigliana (Provincia di Torino) e sul suo substrato cristallino. Memorie della Societa` Italiana di Scienze Naturali e del Museo Civico di Storia Naturale di Milano, 18, p.95-168.

Pettersson, K., Grust, K., Weyhenmeyer, G., Blenckner, T. 2003. Seasonality of chlorophyll and nutrients in Lake Erken – effects of weather conditions. Hydrobiologia 506–509, p.75–81.

Pott, R. 1998. Effects of human interference on the landscape with special reference to the role of grazing livestock. In WallisDeVries, M. F., Bakker, J. P., van Wieren, S. E., editors, Grazing and Conservation Management, Kluwer Academic Publishers, Dordrecht, p.107-136.

Rodbell, D. T. 2000. Cold, Cold, Everywhere ? Science, New Series, Vol. 290, No. 5490 (Oct. 13), p.285-286.

Rottoli, M., Castiglioni, E. 2009. Prehistory of plant growing and collecting in northern Italy, based on seed remains from the early Neolithic to the Chalcolithic (c. 5600-2100 cal B.C.). Veget Hist Archaeobot, 18, p.91-103.

Ruddiman, W. F. 2001. Earth's Climate: Past and Future. W.H. Freeman and Company, New York. 2001.

Sandgren, P., Snowball, I. 2001. Application of mineral magnetic techniques to paleolimnology. In Last, W.M., Smol, J.P. editors, Tracking Environmental Change Using Lake Sediments, vol. 2, Kluwer Academic Publishers, Dordrecht, p.217-237.

Schelske, C. L., Stoermer, E. F., Conley, D. J., Robbins, J. A., Glover, R. M. 1983. Early Eutrophication in the Lower Great Lakes: New Evidence from Biogenic Silica in Sediments. Science, New Series, Vol. 222, No. 4621 (Oct. 21), p.320-322.

Schindler, D. W., Bayley, S. E., Parker, B. R., Beaty, K. G., Cruickshank, D. R., Fee, E. J., Schindler, E. U., Stainton, M. P. 1996. The effects of climatic warming on the properties of boreal lakes and streams at the Experimental Lakes Area, northwestern Ontario. Limnol. Oceanogr., 41 (5), p.1004-1017.

Smol, J.P., Boucherle, M.M. 1985. Postglacial changes in algal and cladoceran assemblages in Little Round Lake, Ontario. Arch. Hydrobiol. 103: 25–49.



Smol, J.P. 2008. *Pollution of Lakes and Rivers: A Paleoenvironmental Perspective*. 2nd Edition. Blackwell Publishing, Oxford. 383 pp.

Starkel, L. 1991. Environmental changes at the Younger Dryas - Preboreal Transition and during the early Holocene: some distinctive aspects in central Europe. *The Holocene* 1, 3 p.234-242.

Stockner, J.G., Benson, W.W. 1967. The succession of diatom assemblages in the recent sediments of Lake Washington. *Limnology and Oceanography*, 12, p.513-32.

Sugita, S., MacDonald, G. M., Larsen, C. P. S. 1997 Reconstruction of FIRE disturbance and forest sucesión from fósil pollen in lake sediments: potential and limitations. In eds Clark, J. S., Cachier, H., Goldammer, J. G., Stocks, B. *Sediment Records of Biomass Burning and Global Change*, vol 51, p.387-412. NATO ASI Series I: Global Enviromental Change. Springer, Berlin, Germany.

Sugita, S., Gaillard, M. J., Broström, A. 1999. Landscape openness and pollen records: a simulation approach. *The Holocene* 9, 4, p.409–421.

Sugita, S. 2007. Theory of quantitative reconstruction of vegetation I: pollen from large sites REVEALS regional vegetation. *The Holocene* 17 (2), p.229–241.

ter Braak, C.J.F., Juggins, S. 1993. Weighted averaging partial least squares regression (WA-PLS): an improved method for reconstructing environmental variables from species assemblages. *Hydrobiologia*, 269/270, p.485-502.

ter Braak, C. J. F., Juggins, S., Birks, H. J. B., & van der Voet, H. 1993. *Weighted averaging partial least squares regression (WA-PLS): definition and comparison with other methods for species-environmental calibration*, Elsevier Science Publishers, Amsterdam.

ter Braak, C. J. F., Prentice, I. C. 1988. A theory of gradient analysis. *Advances in Ecological Research*, 18, p.271-317.

Thompson, J. B., Schultze-Lam, S., Beveridge, T. J., Des Marais, D. J. 1997. Whiting Events: Biogenic Origin Due to the Photosynthetic Activity of Cyanobacterial Picoplankton. *Limnology and Oceanography*, Vol. 42, No. 1 (Jan.), p.133-141.

Tilman, D., Kilham, S. S., Kilham, P. 1982. Phytoplankton Community Ecology: The Role of Limiting Nutrients. *Annual Review of Ecology and Systematics*, 13, p.349-372.

Tinner, W., Hubschmid, P., Wehrli, M., Ammann, B., Conedera, M. 1999. Long-Term Forest Fire Ecology and Dynamics in Southern Switzerland. *Journal of Ecology*, Vol. 87, No. 2 (Apr.), p.273-289.

Tinner, W., Conedera, M., Gobet, E., Hubschmid, P., Wehrli, M., Ammann, B. 2000. A palaeoecological attempt to classify fire sensitivity of trees in the southern Alps. *The Holocene*, 10(5), p.565-574.

Tinner, W., Lotter, A. F. 2001. Central European vegetation response to abrupt climate change at 8.2 ka. *Geology*, 29, p.551-554.

Tinner, W., Hu, F.S. 2003. Size parameters, size-class distribution and area-number relationship of microscopic charcoal: relevance for fire reconstruction. *The Holocene*, 13, p.291-296.

Tinner, W., Hofstetter, S., Zeugin, F., Conedera, M., Wohlgemuth, T., Zimmermann, L., Zweifel, R. 2006. Long-distance transport of macroscopic charcoal by an intensive crown fire in the Swiss Alps - implications for fire history reconstruction. *The Holocene*, 16, 2, p.287-292.

Tinner, W., Lotter, A. F. 2006. Holocene expansions of *Fagus sylvatica* and *Abies alba* in Central Europe: where are we after eight decades of debate? *Quaternary Science Reviews*, 25, p.526-549.

Tippett, R. 1964. An investigation into the nature of the layering of deep-water sediments in two eastern Ontario lakes. *Can. J. Bot.*, 42, p.1693-1709.

Tolotti, M., Corradini, F., Boscaini, A., Calliari, D. 2007. Weather-driven ecology of planktonic diatoms in Lake Tovel (Trentino, Italy) *Hydrobiologia*, 578, p.147-156.

Valsecchi, V., Finsinger, W., Tinner, W., Ammann, B. 2008. Testing the influence of climate, human impact and fire on the Holocene population expansion of *Fagus sylvatica* in the southern Prealps (Italy). *The Holocene*, 18 (4) p.603-614.

Valsecchi, V., Tinner, W., Finsinger, W., Ammann, B. 2006. Human impact during the Bronze Age on the vegetation at Lago Lucone (northern Italy). *Veget Hist Archaeobot*, 15, p.99-113.

Vollweiler, N., Scholz, D., Mühlinghaus, C., Mangini, A., Spötl, C. 2006. A precisely dated climate record for the last 9 kyr from three high alpine stalagmites, Spannagel Cave, Austria. *Geophys Res Let*, 33, L20703

Watts, W. A. 1973. Rates of change and stability in vegetation in the perspective of long periods of time. In Birks, H.J.B. and West, R.G., editors, *Quaternary plant ecology*, Blackwell, p.195-206.

Whiteside, M. C. 1983. The mythical concept of eutrophication. *Hydrobiologia*, 103, p.107-111.

Whitlock, C., Larsen, C. P. S., 2002. Charcoal as a fire proxy. In: Smol, J.P., Birks, H.J.B., Last, W.M. (Eds.), *Tracking Environmental Change Using Lake Sediments*, vol. 3: Terrestrial, Algal, and Siliceous Indicators. Kluwer Academic Publishers, Dordrecht, The Netherlands, p.74–97.